Neurobiology of Disease 127 (2019) 163–177

Contents lists available at ScienceDirect

Neurobiology of Disease

journal homepage: www.elsevier.com/locate/ynbdi

Systemic peptide mediated delivery of an siRNA targeting α-syn in the CNS ameliorates the neurodegenerative process in a transgenic model of Lewy body disease

Brian Spencer[a], Ivy Trinh[a], Edward Rockenstein[a], Michael Mante[a], Jazmin Florio[a], Anthony Adame[a], Omar M.A. El-Agnaf[b], Changyoun Kim[c], Eliezer Masliah[a,c,d], Robert A. Rissman[a,e,*]

[a] Department of Neurosciences, University of California, San Diego, La Jolla, CA, USA
[b] Neurological Disorders Center, Qatar Biomedical Research Institute, Hamad Bin Khalifa University, Doha, Qatar
[c] Laboratory of Neurogenetics National Institute on Aging, National Institutes of Health, Bethesda, MD, USA
[d] Division of Neuroscience, National Institute on Aging, National Institutes of Health, Bethesda, MD, USA
[e] Veterans Affairs San Diego Healthcare System San Diego, CA, USA

ARTICLE INFO

Keywords:
Parkinson's disease
siRNA
Blood-brain barrier
α-Synuclein
Low density lipoprotein receptor
Apolipoprotein B
Receptor mediated transytosis

ABSTRACT

Neurodegenerative disorders of the aging population are characterized by progressive accumulation of neuronal proteins such as α-synuclein (α-syn) in Parkinson's Disease (PD) and Amyloid ß (Aß) and Tau in Alzheimer's disease (AD) for which no treatments are currently available. The ability to regulate the expression at the gene transcription level would be beneficial for reducing the accumulation of these proteins or regulating expression levels of other genes in the CNS. Short interfering RNA molecules can bind specifically to target RNAs and deliver them for degradation. This approach has shown promise therapeutically *in vitro* and *in vivo* in mouse models of PD and AD and other neurological disorders; however, delivery of the siRNA to the CNS *in vivo* has been achieved primarily through intra-cerebral or intra-thecal injections that may be less amenable for clinical translation; therefore, alternative approaches for delivery of siRNAs to the brain is needed. Recently, we described a small peptide from the envelope protein of the rabies virus (C2-9r) that was utilized to deliver an siRNA targeting α-syn across the blood brain barrier (BBB) following intravenous injection. This approach showed reduced expression of α-syn and neuroprotection in a toxic mouse model of PD. However, since receptor-mediated delivery is potentially saturable, each allowing the delivery of a limited number of molecules, we identified an alternative peptide for the transport of nucleotides across the BBB based on the apolipoprotein B (apoB) protein targeted to the family of low-density lipoprotein receptors (LDL-R). We used an 11-amino acid sequence from the apoB protein ($ApoB^{11}$) that, when coupled with a 9-amino acid arginine linker, can transport siRNAs across the BBB to neuronal and glial cells. To examine the value of this peptide mediated oligonucleotide delivery system for PD, we delivered an siRNA targeting the α-syn (siα-syn) in a transgenic mouse model of PD. We found that $ApoB^{11}$ was effective (comparable to C2-9r) at mediating the delivery of siα-syn into the CNS, co-localized to neurons and glial cells and reduced levels of α-syn protein translation and accumulation. Delivery of $ApoB^{11}$/siα-syn was accompanied by protection from degeneration of selected neuronal populations in the neocortex, limbic system and striato-nigral system and reduced neuro-inflammation. Taken together, these results suggest that systemic delivery of oligonucleotides targeting α-syn using $ApoB^{11}$ might be an interesting alternative strategy worth considering for the experimental treatment of synucleinopathies.

Abbreviations: α-syn, α-synuclein; LBD, Lewy body disease; PD, Parkinson's Disease; DLB, Dementia with Lewy bodies; Aβ, Amyloid β; AD, Alzheimer's disease; Htt, huntingtin; HD, Huntington's Disease; FTD, Fronto-temporal dementia; ALS, Amyotrophic lateral sclerosis; BBB, blood-brain barrier; CMT, carrier mediated transporters; RMT, receptor mediated transport; LDL-R, low-density lipoprotein receptor; siα-syn, siRNA targeting α-syn; C2-9r, small peptide from the envelope protein of the rabies virus; ApoB, apolipoprotein B; si-sc, si-scrambled (sc) RNA; $ApoB^{11}$, 11-amino acid sequence from the apoB protein coupled with a 9-amino acid arginine linker

* Corresponding author at: Department of Neurosciences, University of California, San Diego, La Jolla, CA, USA.
E-mail address: rrissman@ucsd.edu (R.A. Rissman).

https://doi.org/10.1016/j.nbd.2019.03.001
Received 26 December 2018; Received in revised form 5 February 2019; Accepted 4 March 2019
Available online 05 March 2019
0969-9961/ Published by Elsevier Inc.

1. Introduction

Neurodegenerative disorders of the aging population are characterized by progressive accumulation of neuronal proteins such as α-synuclein (α-syn) in Lewy body disease (LBD) (including Parkinson's Disease (PD) and Dementia with Lewy bodies (DLB)) (McKeith et al., 2017), Amyloid β (Aß) and Tau in Alzheimer's disease (AD) (De Strooper and Karran, 2016; Gibbons et al., 2018; Selkoe and Hardy, 2016), huntingtin (Htt) in Huntington's Disease (HD) (Margulis and Finkbeiner, 2014) and TDP43 in Fronto-temporal dementia (FTD) and Amyotrophic lateral sclerosis (ALS) (Cairns et al., 2007; Lee et al., 2011a). This is accompanied by death of selected neuronal populations and neuro-inflammation leading to cognitive impairment, parkinsonism and motoric disorders for which no treatments are currently available (Fu et al., 2018). The mechanisms of neurodegeneration are not fully understood but involve toxicity mediated by oligomeric forms and other multimers of the aggregating (Gibbons et al., 2018; Lashuel et al., 2013; Mucke and Selkoe, 2012) as well as cell to cell propagation (Gibbons et al., 2018; Jucker and Walker, 2018; Lee et al., 2011b; Liu et al., 2012) of the accumulating protein. It is believed that accumulation of proteins such as α-syn, Aß, Tau, Htt and TDP43 might be the result of a disequilibrium between the levels of synthesis, clearance and folding of these proteins (Brettschneider et al., 2015; Lashuel et al., 2013). Therefore, therapeutic strategies might involve decreasing synthesis, increasing clearance or promoting proper folding of these proteins (Valera et al., 2016a; Valera et al., 2016b). There has been progress in developing strategies to decrease the synthesis of proteins involved in neurological disorders by utilizing anti-sense oligonucleotides (Ghosh and Tabrizi, 2017; Schoch and Miller, 2017). Clinical trials are now underway with anti-sense oligonucleotides in HD (Dickey and La Spada, 2018; Ghosh and Tabrizi, 2017; Keiser et al., 2016) and similar strategies are being explored for PD and AD targeting α-syn (Alarcon-Aris et al., 2018) and Tau (Crunkhorn, 2017; DeVos and Hyman, 2017; Vossel et al., 2010). In addition to anti-sense, another approach for reducing gene expression includes the use of short interfering RNA (siRNA) oligonucleotides that can bind specifically to target RNAs and target them for degradation *via* the RISC complex have been proposed for the treatment of neurodegenerative disorders (Alves et al., 2016; Koutsilieri et al., 2007; Magen and Hornstein, 2014; White and Mallucci, 2009). This approach has shown promise as a therapeutic *in vitro* (Kao et al., 2004; Liu et al., 2008; Luo et al., 2004) and in mouse models of PD (Zharikov et al., 2015) and AD and other neurological disorders (Chang et al., 2018; Singer et al., 2005; Xilouri et al., 2016); however, as with anti-sense, delivery of the siRNA to the CNS *in vivo* is challenging and so far has been achieved primarily through intra-thecal and intra-cranial injections. Thus, the need to develop less invasive systemic approaches to deliver oligonucleotides into the CNS and across the blood-brain barrier (BBB).

The BBB controls the passage of substances from the blood into the central nervous system. Small molecules (400–500 Da) can pass freely (Lipinski et al., 2001); however, larger molecules are actively transported across the BBB *via* three main mechanisms: (a) carrier mediated transporters (CMT) allow the transport of nutrients such as sugars and amino acids from blood to the brain, (b) receptor mediated transport (RMT) allows the transport of larger proteins and carrier proteins such as transferrin (iron), apolipoprotein (lipids) and insulin from the blood to the brain, and (c) efflux transporters export drugs from the CNS to the blood *e.g.* p-glycoprotein and breast cancer resistance protein (Abbott et al., 2006; Begley, 2004; Begley and Brightman, 2003). Thus, a major challenge for the systemic delivery of oligonucleotides for neurodegenerative diseases is the transport to the CNS.

In the past few years, a number of receptor mediated methods to deliver oligonucleotides and peptides have been tested (Pardridge, 2017) including the use of the transferrin (Pardridge, 2016), insulin (Lajoie and Shusta, 2015) and low-density lipoprotein (LDL-R) receptors (Masliah and Spencer, 2015a; Spencer and Verma, 2007). Recently, we described a small peptide from the envelope protein of the rabies virus (C2-9r) that was utilized to deliver an siRNA targeting α-syn (siα-syn) across the BBB following systemic injection (Javed et al., 2016). With this approach, we showed reduced expression of α-syn in various brain regions and protection of the nigro-striatal system from the neurotoxic effects of MPTP in a mouse model of PD (Javed et al., 2016).

In this study we have identified an alternative peptide for the transport of nucleotides across the BBB based on the apolipoprotein B (ApoB) protein targeted to the family of LDL-R (Masliah and Spencer, 2015b; Spencer and Verma, 2007). For previous studies we utilized a 38 aa peptide (Spencer et al., 2018; Spencer et al., 2014a; Spencer et al., 2016c; Spencer et al., 2015; Spencer et al., 2014b) expressed from a lentiviral vector while for the present study we used a reduced 11-amino acid sequence from the apoB protein ($ApoB^{11}$) protein, coupled with a 9-amino acid arginine linker for transporting siRNAs across the BBB to neuronal and glial cells following intra-peritoneal injection. We tested the effectiveness of this approach by delivering an siRNA targeting α-syn (siα-syn) into an α-syn tg mouse model of PD/DLB and showed reduced accumulation of α-syn associated with amelioration of the neurodegenerative and inflammatory pathology. Taken together, these results support the notion that systemic delivery of oligonucleotides targeting α-syn using $ApoB^{11}$ might be an alternative strategy worth considering when developing experimental treatments for synucleinopathies of the aging population such as PD and DLB.

2. Results

2.1. An 11-amino acid peptide from Apolipoprotein B can deliver an siRNA to neurons and reduces α-synuclein levels in vitro

α-synuclein is a 140 amino acid synaptic protein (Iwai et al., 1995; Valera and Masliah, 2013) that plays a role as a scaffolding protein in vesicle trafficking, dopamine release and synaptic remodeling (Chandra et al., 2004). Misfolded, aggregated α-syn has been implicated in neurological disorders with parkinsonism including PD, DLB and MSA (Reviewed in (Eller and Williams, 2011)). Given the neuronal toxicity of α-syn accumulation, therapeutic strategies for synucleinopathies might include reducing expression of the mRNA through siRNA. We have previously described a small peptide from the envelope protein of the rabies virus (C2-9r) that can be used systemically to deliver siα-syn into the CNS (Javed et al., 2016). However, the rhabdovirus receptor saturates rapidly (Wunner et al., 1984), thus for this study we investigated the usefulness of ApoB as an alternative carrier protein. This is based on our previous studies showing delivery of protein and peptides to the CNS by receptor mediated transcytosis across the BBB with the LDL-R using a 38-amino acid receptor binding domain from apolipoprotein B ($ApoB^{38}$) (Spencer et al., 2014a; Spencer et al., 2011; Spencer et al., 2016c; Spencer et al., 2015; Spencer et al., 2014b; Spencer and Verma, 2007). Based on literature review (Knott et al., 1986; Yang et al., 1986), we identified an 11-amino acid core domain that represented the putative minimal receptor binding domain ($ApoB^{11}$) (Fig. 1A). For delivery of oligonucleotides, we added 5 Gly (G) and 9 Arg (R) amino acids to the C-terminus (Javed et al., 2016). The glycine residues act as flexible anchor and the 9 arginine residues are a positively charged tail for binding negatively charged nucleotides (Fig. 1A).

To determine the ratio between the $ApoB^{11}$ peptide and RNA that leads to complete complex formation, 100 nM of siRNA was incubated with increasing molar ratios of $ApoB^{11}$ and run on an agarose gel. Excess RNA that was not completely bound to and charge neutralized by the 9 arginine residues of the $ApoB^{11}$ peptide would enter the gel and be visible by ethidium bromide staining. At a ratio of 1:0 and 1:1, unbound RNA is observable in the gel; however, at a ratio of 1:10 (0 .1μM siRNA: 1 μM $ApoB^{11}$), there is no free RNA to enter the gel suggesting that all the charged RNA is neutralized by the arginine

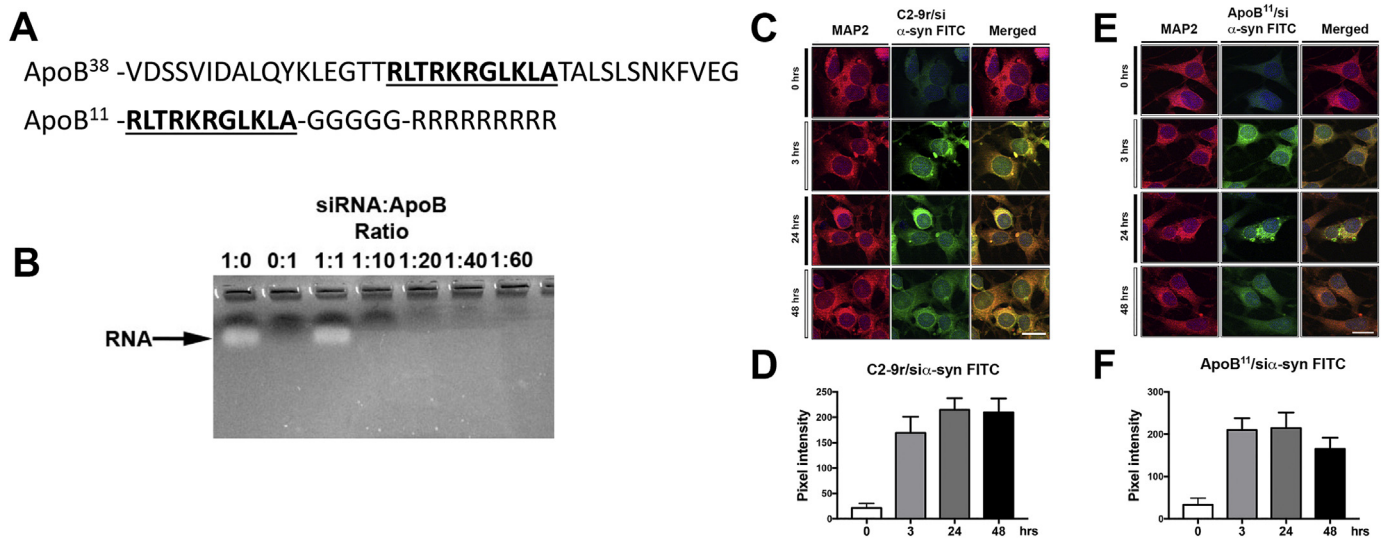

Fig. 1. Characteristics of a non-viral peptide derived from ApoB that delivers a short RNA targeting α-syn to neuronal cells. (A) Diagrammatic illustration of the original 38-amino acid peptide derived from the Apolipoprotein B protein for delivery of proteins and peptides for receptor mediated BBB transcytosis to the CNS and the novel shorter, 11 amino acid (underlined) fragment coupled to a 5 Glycine linker and a 9 Arginine positively charged tail utilized for delivering siRNA into neuronal cells. (B) The siRNA targeting α-syn was incubated with different molar ratios of the ApoB^{11} peptide for 30 min. Complexed RNA and protein were run through an agarose gel and unconjugated RNA was observed by ethidium bromide staining. (C, E) Immunocytochemical and laser scanning microscopy analysis of N2A mouse neuronal cells incubated with FITC labeled siRNA targeting α-syn added at a ratio of 1:40 siRNA:C2-9r (derived from rhabdovirus positive control) or 1:10 siRNA:ApoB^{11} (respectively) and analyzed at different time points for uptake of the FITC labeled siRNA. Neuronal cells were labeled with an antibody against MAP2 and visualized with Tyramide Red. (D, F) Fluorescence levels representative of FITC tagged siRNA:C2-9r or siRNA:ApoB^{11} (respectively) trafficking into neuronal cells were estimated after 3, 24 and 48 h post incubation and expressed as pixel intensity. Levels rapidly increased and plateau after 3 h. Scale bar represents 15 μm. (For interpretation of the references to colour in this figure legend, the reader is referred to the web version of this article.)

residues of the ApoB^{11} vector (Fig. 1B). For future applications, we used a ratio of 1:10 when incubating the siRNA and ApoB^{11} vector prior to applications.

To ascertain if the ApoB^{11} peptide could deliver siRNA in a comparable manner to the recently published BBB transport peptide derived from the Rabies G envelope protein (C2-9r), the N2A mouse cholinergic neuronal cells were incubated for various time points with the C2-9r peptide with a FITC labeled siRNA targeting a conserved sequence on mouse and human α-syn (siα-syn) (Spencer et al., 2016a) at a ratio of 1:40 as previously published (Javed et al., 2016), while we incubated the FITC-siRNA with the ApoB^{11} vector at a molar ratio of 1:10 *in vitro* and then added the vector to differentiated N2A neuronal cells. Compared to controls, the C2-9r/siα-syn FITC was detected at 3 h and plateaued at 48 to 72 h (Fig. 1C, D). Similarly, for the ApoB^{11} vector, delivery to neuronal cells was detected shortly after incubation with the ApoB^{11}/siα-syn FITC complex, FITC label was observed throughout the cytoplasm in the neuronal cells beginning at 3 h post-incubation (Fig. 1E, F). The FITC signal appeared to become more punctate by 24 h and at 48 h was beginning to diminish indicating a degradation of either the FITC signal or the siRNA (Fig. 1E, F).

Next, we investigated the time course and differential effects of the C2-9r and ApoB^{11} vectors delivering the siα-syn into neurons and modulating α-syn levels. Consistent with a previous study (Javed et al., 2016), treatment of N2A cells with the C2-9r/siα-syn resulted in a time dependent 25% and 80% reduction in α-syn at 24 h and 48–72 h respectively (Fig. 2A, B). Likewise, treatment with the ApoB^{11}/siα–syn reduced the accumulation of α-syn in a time dependent manner with 30% reduction at 24–48 h after treatment and nearly complete elimination of α-syn signal by immunocytochemistry at 72 h (Fig. 2C, D). This was corroborated in a similar experiment where total protein was extracted and α-syn examined by immunoblot (Fig. 2E, F). At 24 h post-treatment, α-syn levels was approximately 30% (C2-9r) – 35% (ApoB^{11}) of control levels, while at 48 h the levels of α-syn were reduced by 70% (Fig. 2F). Together, these results support the notion that ApoB^{11}/siα-syn is as effective as the C2-9r at delivering siα-syn and reducing expression, providing support for evaluating this ApoB^{11}/siα-syn *in vivo*.

2.2. Systemically administered ApoB^{11} and C2-9r vectors deliver siRNA to neurons and glial cells in non-tg and α-syn tg mice

We have previously delivered peptides and proteins across the BBB following intra-peritoneal injections when they are fused to a 38-amino acid LDL-R binding domain of ApoB (Spencer et al., 2018; Spencer et al., 2014a; Spencer et al., 2016c; Spencer et al., 2015; Spencer et al., 2014b). In contrast, experiments delivering C2-9r/siα-syn were performed following intra-venous injection (Javed et al., 2016). Therefore, we performed preliminary experiments with FITC labeled siRNA conjugated to either ApoB^{11} or C2-9r delivered to non-tg mouse by either intra-venous or intra-peritoneal injection. Four hours post intra-venous injection we found that compared to the siRNA-FITC alone, the siRNA conjugated to C2-9r or ApoB^{11} co-localized with 65% of NeuN positive neurons (Fig. 3A, B). Along these lines, following intra-peritoneal injection the siRNA-FITC conjugated to C2-9r or ApoB^{11} co-localized with 55% of NeuN positive neurons (Fig. 3C, D). Due to the ease of intra-peritoneal injection, for subsequent experiments, intra-peritoneal delivery was chosen for the route of administration.

To determine if the peptides could transport siRNA across the BBB following intra-peritoneal delivery in both non-tg and α-syn tg mice, animals were treated with either C2-9r /siα-syn FITC, ApoB^{11}/siα-syn FITC or naked siα-syn FITC. Compared to mice treated with siα-syn FITC, 4 h after systemic injection, both the C2-9r and ApoB^{11} delivered FITC tagged siα-syn was detected in neuronal cells as shown by co-labeling with the neuronal marker NeuN, both in the brains of non-tg (Fig. 4A) and α-syn tg mice (Fig. 4B). Labeling was primarily peri-nuclear in punctate patterns but was also nuclear (Fig. 4A, B). Interestingly, while the C2-9r co-localized with approximately 40% of NeuN positive cells in non-tg and α-syn tg mice, the ApoB^{11} siRNA was present in approximately 55 and 60% of the NeuN positive neurons in non-tg and α-syn tg mice respectively, with the difference reaching

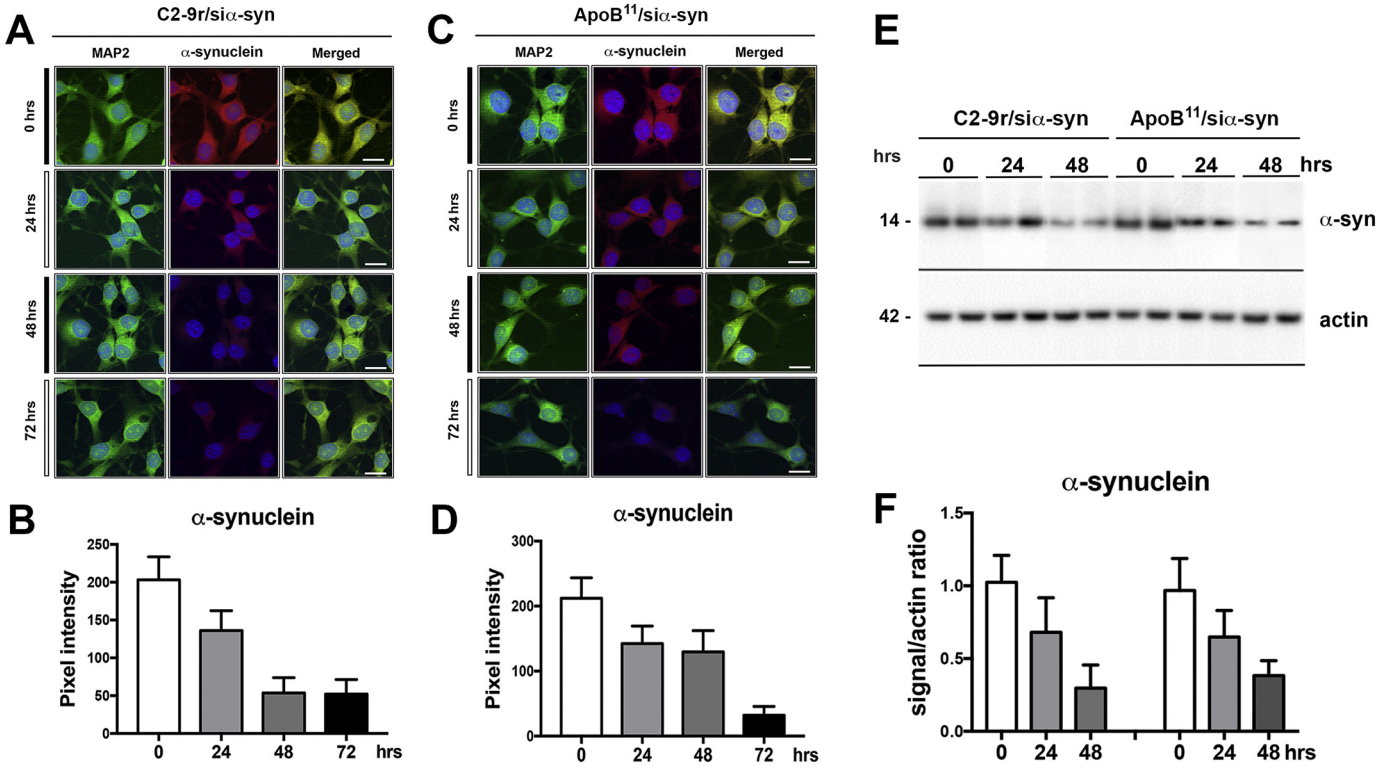

Fig. 2. Analysis of levels of α-syn following delivery of ApoB^{11}siRNA targeting α-syn in neuronal cells *in vitro*. (A) N2A neuronal cells were treated with 100 pmol siα-syn conjugated to the (A) C2-9r peptide (derived from rhabdovirus, positive control) or to the (C) ApoB^{11} peptide and double immunostained with antibodies against α-syn (red) and the neuronal marker MAP2 (FITC) and analyzed with the laser confocal microscope. (B, D) Fluorescence levels representative of α-syn immunoreactivity expressed as pixel intensity following 24, 48 and 72 h. Levels of α-syn immunostaining started to decrease after 24 h reaching maximum effects after 48 h with the C2-9r/siα-syn and 72 h with the ApoB^{11}/siα-syn. (E) Representative immunoblot from replicate from N2A neuronal cells treated with siα-syn conjugated to the C2-9r peptide or the ApoB^{11} peptides after 24 and 48 h. (F) Image analysis of the levels of α-syn immunoreactive band at 14 kDa as a ratio to ß-actin after 24 and 48 h. Scale bar represents 10 μm. (For interpretation of the references to colour in this figure legend, the reader is referred to the web version of this article.)

significance in the α-syn tg group (Fig. 4C). No labeling was observed in neuronal cells in the mice treated with FITC tagged naked siRNA (Fig. 4C). Moreover, compared to mice treated with siα-syn FITC alone, after intra-peritoneal injection, both the C2-9r/ and ApoB^{11}/siα-syn FITC localized to approximately 20–25% of astrocytes as shown by co-labeling with the astroglial cell marker GFAP, both in the brains of non-tg (Fig. 4D, F) and α-syn tg mice (Fig. 4E, F). No labeling was observed in astroglial cells in the mice treated with FITC tagged naked siRNA (Fig. 4F).

Next, we investigated the co-localization of the C2-9r /siα-syn FITC and ApoB^{11}/siα-syn FITC to neurons accumulating α-syn. For this purpose, co-labeling experiments were performed with the Syn-1 antibody that cross reacts with mouse and human α-syn since the siRNA chosen for these experiments also recognizes both species. Compared to the siα-syn FITC alone, both the C2-9r and ApoB^{11} delivered FITC tagged siα-syn was detected in the brains of non-tg (Fig. 4G) and α-syn tg mice (Fig. 4H). In the non-tg mice, α-syn was detected in the neuropil with a punctate pattern and co-localized to a low extent with the C2-9r and ApoB^{11} (Fig. 4I). In contrast, in the α-syn tg mice, α-syn immunostaining concentrated in the cell bodies reflecting the abnormal accumulation of this synaptic protein in the tg mice (Fig. 4H). As expected no signal or co-localization was observed in tg mice treated with siα-syn FITC alone (Fig. 4H, I); however, in α-syn tg mice treated with C2-9r /siα-syn FITC or ApoB^{11}/siα-syn FITC, there was close co-localization to neurons exhibiting α-syn accumulation (Fig. 4H, I).

Together, these studies indicate that similar to C2-9r, the ApoB^{11} vector is capable of delivering the siα-syn across the BBB to α-syn expressing cells, reaching the correct target.

2.3. ApoB^{11} and C2-9r mediated delivery of siRNA reduces α-syn accumulation in α-syn tg mice

We have previously shown that systemic delivery of siRNA targeting α-syn with the C2-9r peptide protects wild-type mice from the neurotoxic effects of MPTP (Javed et al., 2016), so for the present study, the objective was to evaluate the neuroprotective effects following systemic delivery of C2-9r and the novel peptide ApoB^{11} in an α-syn tg model of synucleinopathy. For this purpose, non-tg and PDGF/α-syn tg mice were treated with either si-scrambled (sc) RNA or siα-syn conjugated with either ApoB^{11} or C2-9r peptides. The si-sc was an RNA with the same ratio of nucleotides as the siα-syn and incubated at the same ratio of 1:10 with ApoB^{11} or 1:40 with C2-9r *in vitro* prior to *in vivo* delivery. Mice were treated twice weekly for 4 weeks by intraperitoneal injection of either C2-9r or ApoB^{11}/siα-syn or si-sc.

Since the siα-syn that we designed targets both mouse and human α-syn (Fig. 2), we evaluated the effects of the C2-9r and ApoB^{11} vectors carrying si-sc or siα-syn on levels of α-syn accumulation using the Syn-1 antibody against total α-syn. As expected, in the non-tg mice treated with either the C2-9r or ApoB^{11} si-sc, α-syn was detected with a punctuate pattern in the neuropil in multiple brain regions with the highest levels detected in the hippocampus (Fig. 5A, upper two panels). Compared to the C2-9r or ApoB^{11} si-sc group (Fig. 5A, upper panel), in non-tg mice treated with either the C2-9r or ApoB^{11} siα-syn there was a 45–50% reduction in the levels of α-syn immunoreactivity in the neocortex (Fig. 5B), hippocampus (Fig. 5C) and striatum (Fig. 5D). In the α-syn tg mice treated with si-sc there was abundant accumulation of α-syn in neuropil and neuronal cell bodies in the neocortex, hippocampus and striatum (Fig. 5A, lower 3rd and 5th panels), with the neocortex

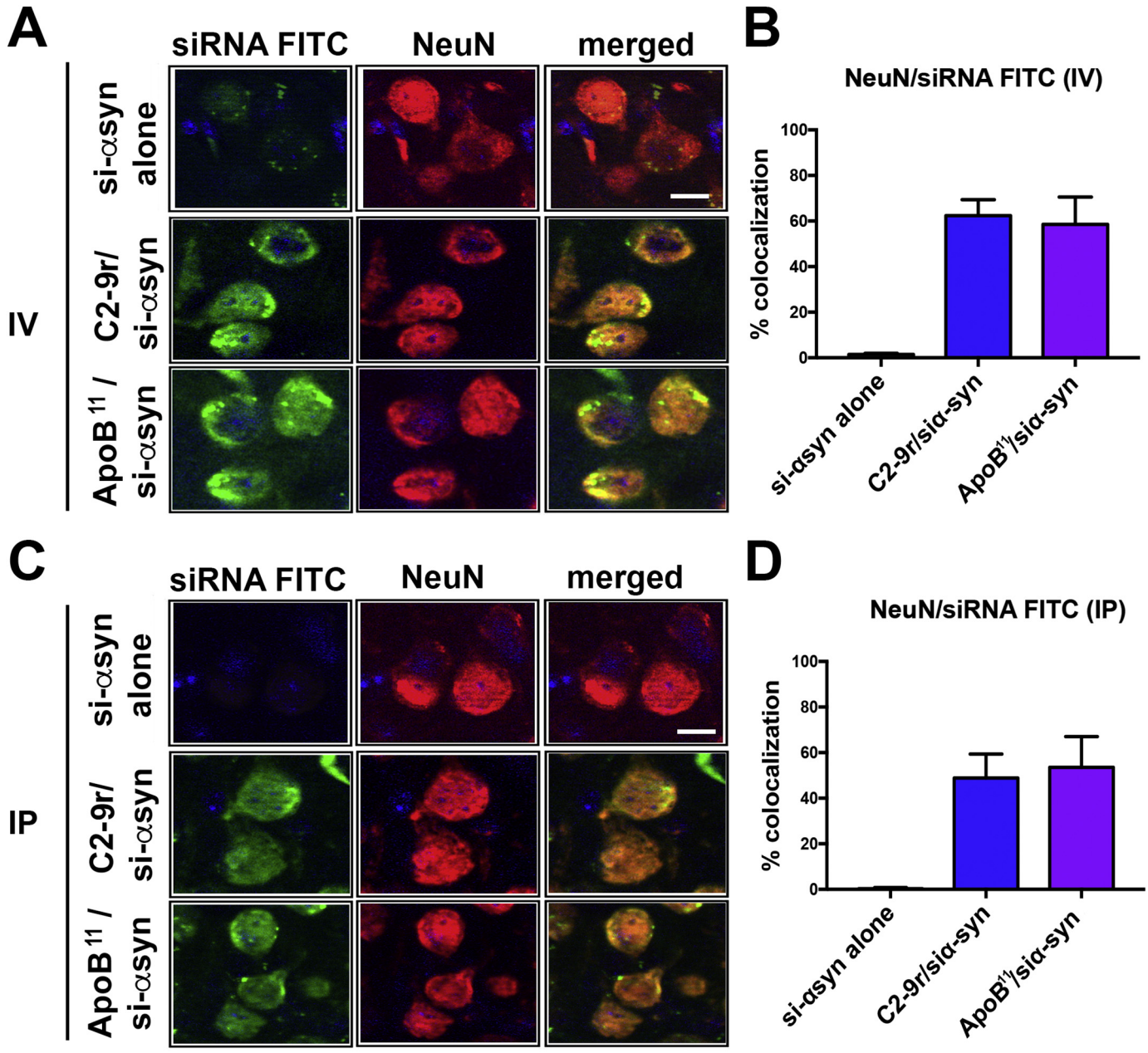

Fig. 3. Comparison of the levels of the peptide-siRNA α-syn in the mouse brain following intra-venous or intra-peritoneal delivery. Non-tg mice received a single intra-venous (IV) or intra-peritoneal (IP) injection of FITC labeled α-syn siRNA (si-αsyn) conjugated to either C2-9r, ApoB^{11} or naked siRNA (si-αsyn alone), 4 h after injection, mice were sacrificed, whole brain removed, fixed and sections immunolabeled with an antibody against the neuronal marker NeuN (red). (A) Representative images from the frontal cortex following IV injection of FITC tagged si-αsyn alone or conjugated to C2-9r or ApoB^{11} in sections immunolabeled with NeuN and analyzed with the laser scanning confocal microscope. (B) Image analysis of the sections to estimate the co-localization with between the FITC labeled siRNA (green) and NeuN (red) expressed as % showing very little or no trafficking with the naked siRNA while comparable levels of penetration into neurons *in vivo* with the C2-9r, ApoB^{11} peptides. (C) Representative images from the frontal cortex following IP injection of FITC tagged si-αsyn. (D) Image analysis of the % co-localization between the FITC labeled siRNA (green) and NeuN (red) showing no trafficking of the naked siRNA while high levels of penetration into neurons *in vivo* with the C2-9r, ApoB^{11} peptides. $n = 3$ non-tg (4 m/o) mice per group. Scale bar represents 10 μm. (For interpretation of the references to colour in this figure legend, the reader is referred to the web version of this article.)

and hippocampus displaying higher levels of α-syn accumulation (Fig. 5B, C) compared to the striatum (Fig. 5D). Remarkably, treatment with the C2-9r or ApoB^{11} siα-syn resulted in a 65–70% reduction in the levels of α-syn immunoreactivity in the neocortex (Fig. 5B), 40–50% in the hippocampus (Fig. 6C) and 50–55% in the striatum (Fig. 5D). Overall, treatment with ApoB^{11}/siα-syn displayed a trend toward a greater effect than C2-9r/siα-syn.

Immunoblot analysis of α-syn accumulation in mice treated with the C2-9r or ApoB^{11} siα-syn was done by confirming the results observed by immunohistochemistry (Fig. 6). Compared to the non-tg mice, α-syn tg mice that were treated with the si-sc displayed increased levels of α-syn monomers and multimers in the cytosolic and membrane fractions (Fig. 6A, B). In contrast, in the α-syn tg mice treated with C2-9r or ApoB^{11}/siα-syn there was a 30–40% reduction in the levels of α-syn in the cytosolic and membrane fractions (Fig. 6A, B). We have previously shown that the effects of α-syn reduction might be related to improvements in vesicular transport as α-syn accumulation might interfere with this process as reflected by alterations in Rab3a and Rab5

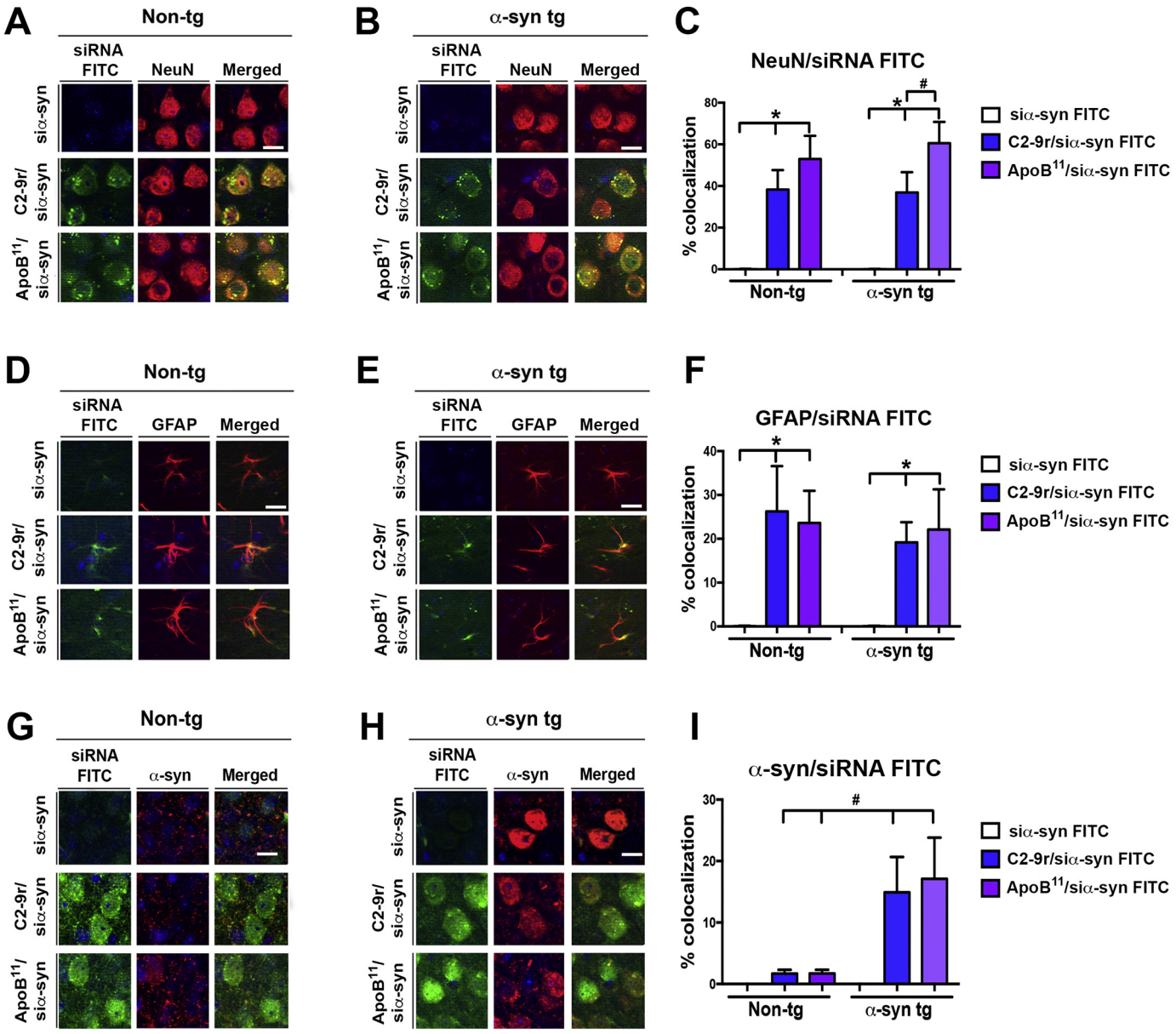

Fig. 4. Cellular distribution of the peptide-siRNA α-syn in the brains of non-transgenic and α-syn transgenic mice following intra-peritoneal injections. Non-tg and α-syn tg mice received a single IP injection of FITC labeled α-syn siRNA (si-αsyn) (green) conjugated to either C2-9r, ApoB^{11} or naked siRNA (si-αsyn alone), 4 h after injection, mice were sacrificed, whole brain removed fixed and sections immunolabeled with antibodies against the neuronal marker NeuN, astroglial cells GFAP and (red) α-syn. (A, B) Representative images of the frontal cortex of non-tg and α-syn tg mice (respectively) following IP injection of FITC tagged si-αsyn alone or conjugated to C2-9r or ApoB^{11} in sections immunostained with NeuN (red) and analyzed with the laser scanning confocal microscope. (C) Image analysis of the sections to estimate the co-localization between the FITC labeled siRNA (green) and NeuN (red) expressed as % showing comparable high levels in neurons *in vivo* with the C2-9r, ApoB^{11} peptides in non-tg and α-syn tg mice. (D, E) Representative images of the frontal cortex of non-tg and α-syn tg mice (respectively) following IP injection of FITC tagged si-αsyn alone or conjugated to C2-9r or ApoB^{11} in sections immunostained with GFAP (red) and analyzed with the laser scanning confocal microscope. (F) Image analysis of the sections to estimate the co-localization between the FITC labeled siRNA (green) and GFAP (red) expressed as % showing comparable colocalization in astroglial cells *in vivo* between the C2-9r or ApoB^{11} peptides in non-tg and α-syn tg mice. (G, H) Representative images of the frontal cortex of non-tg and α-syn tg mice (respectively) following IP injection of FITC tagged si-αsyn alone or conjugated to C2-9r or ApoB^{11} in sections immunostained with α-syn (red) and analyzed with the laser scanning confocal microscope. (F) Image analysis of the sections to estimate the co-localization between the FITC labeled siRNA (green) and α-syn (red) expressed as % showing comparable colocalization in cells with α-syn aggregates *in vivo* between the C2-9r or ApoB^{11} peptides in non-tg and α-syn tg mice. One-way ANOVA with poshoc Dunnet when comparing to control and Tukey-Kramer when comparing in between groups. * indicates statistical significance $p < 0.05$ compared to siRNA alone. # indicates statistical significance $p < 0.05$ compared to C2-9r siRNA. n = 3 non-tg (4 m/o) mice per group. Scale bar represents 10 μm. (For interpretation of the references to colour in this figure legend, the reader is referred to the web version of this article.)

(Spencer et al., 2016a) (Fang et al., 2017). Consistent with these studies, we found that compared to the non-tg mice, in the α-syn tg mice that were treated with the si-sc there were decreased levels of Rab3a and increased levels of Rab5 in the membrane fractions (Fig. 6A, C-D). In contrast, in the α-syn tg mice treated with C2-9r or ApoB^{11}/siα-syn the levels of Rab3a and Rab5 were comparable to those found in the non-tg mice (Fig. 6A, C-D). In summary, both the C2-9r and ApoB^{11}/siα-syn reduced levels of the endogenous and transgene driven (human) α-syn in the brains of the mice that resulted in reduced levels of α-syn aggregates and improvements in vesicular transport proteins.

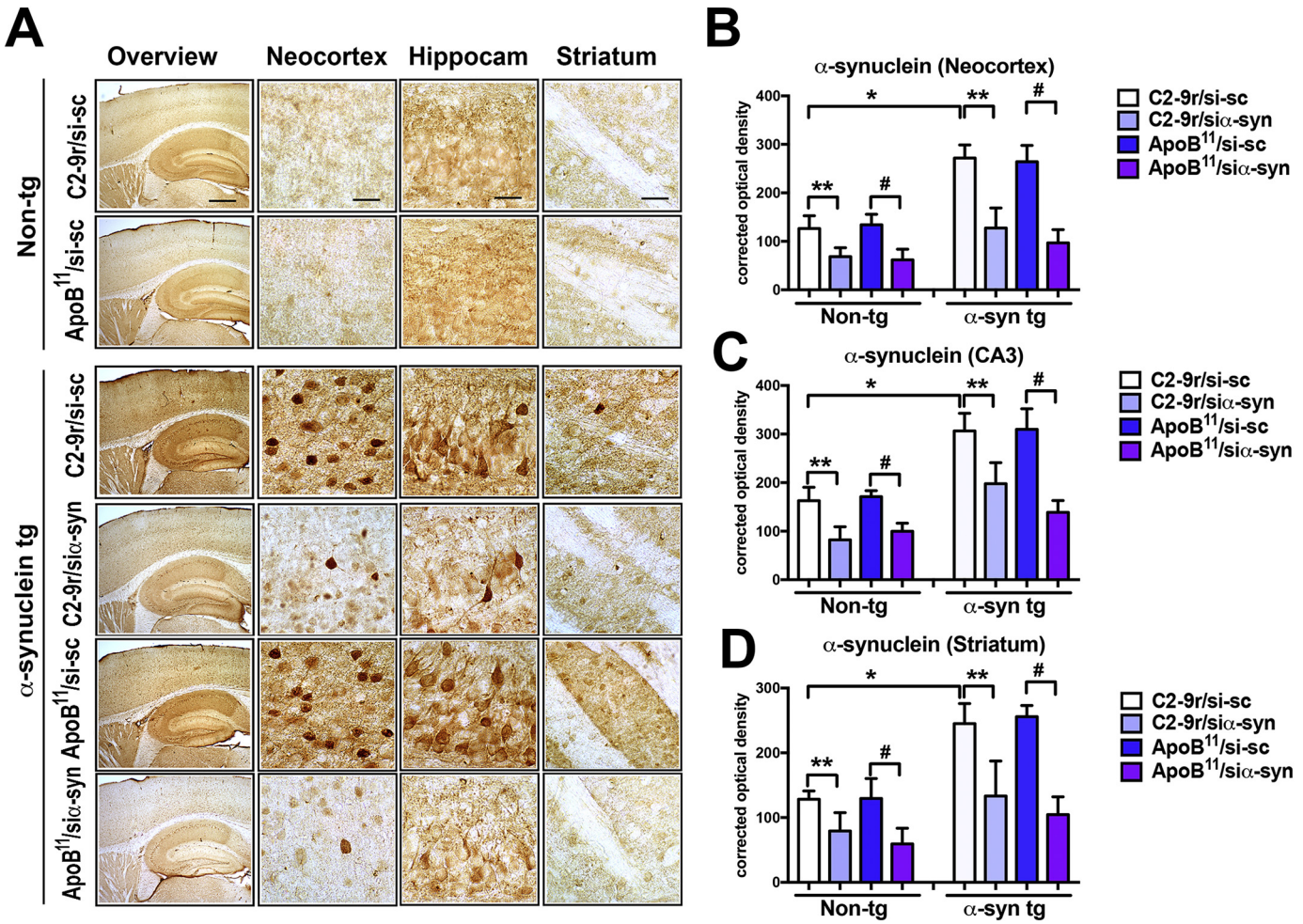

Fig. 5. Immunocytochemical analysis of the effects of systemic delivery of the siα-syn conjugated to C2-9r or ApoB^{11} peptides on accumulation of α-syn in transgenic mice. Four-month-old α-syn tg and non-tg mice received repeated intraperitoneal injections of scrambled siRNA (si-sc) or α-syn siRNA (si-αsyn) conjugated to either C2-9r, ApoB^{11} and were sacrificed 4 weeks later for analysis. Sections were immunolabled with an antibody against FL-α-syn and analyzed by bright field microscopy. (A) Representative images of the neocortex, hippocampus and striatum of non-tg and α-syn tg mice treated with either si-sc or si-αsyn conjugated with C2-9r or ApoB^{11}. Image analysis of levels of expressed as corrected optical density for α-syn immunoreactivity in the (B) neocortex, (C) hippocampus (CA3), and (D) striatum. One-way ANOVA with poshoc Dunnet when comparing to control and Tukey-Kramer when comparing among groups. Statistical significance $p < 0.05$ compared to: * non-tg mice; ** C2-9r/si-sc; # ApoB^{11}/si-sc. Non-tg ($n = 16$) and α-syn tg ($n = 24$). Scale bar represents 250 μm for low magnification panels and 25 μm for higher magnification panels.

2.4. ApoB^{11} and C2-9r mediated delivery of siRNA ameliorates neurodegenerative pathology in α-syn tg mice

Next, we evaluated if reducing the accumulation of α-syn was accompanied by comparable improvements in the neurodegenerative pathology. The PDGF-α-syn tg mice displays neuronal loss and neuroinflammation in the neocortex and hippocampal (CA3) region while the striatum and *S. Nigra* shows little to no change in terms of neuronal loss, but there is considerable loss of TH positive fibers in the striatum (Amschl et al., 2013; Spencer et al., 2014a). To evaluate the effects of modulating α-syn expression in the neurodegenerative pathology in the α-syn tg mice, immunocytochemical analysis was performed with antibodies against the pan-neuronal marker NeuN (Fig. 7) and the marker of the dopaminergic system, TH (Fig. 8). With the antibody against NeuN, in the non-tg mice (Fig. 7, upper panels) no significant differences in the numbers of positive cells were observed in the neocortex (Fig. 7A, B), hippocampus (Fig. 7A, C) or striatum (Fig. 7A, D) when comparing mice treated with C2-9r or ApoB^{11}/si-sc *vs* siα-syn. In contrast and compared to non-tg, the α-syn tg mice treated with C2-9r or ApoB^{11}/si-sc (Fig. 7A, panels in 3rd and 5th rows) displayed a 20–25% decreased numbers of NeuN positive neurons in the neocortex (Fig. 7A, B) and CA3 region of the hippocampus (Fig. 7A, C) but not in the striatum (Fig. 7A, D) as previously reported (Spencer et al., 2014a). Whereas, treatment of α-syn tg mice with the C2-9r or ApoB^{11}/siα-syn ameliorated the loss of NeuN cell in both the neocortex (Fig. 7A, B) and CA3 (Fig. 7A, C) to levels comparable to non-tg mice (Fig. 7A–D). With the antibody against TH, in the non-tg mice (Fig. 8, upper panels) no significant differences in the density of positive fibers were observed in the striatum (Fig. 8A, B), or TH positive neurons in the *S. nigra* (Fig. 8A, C) when comparing mice treated with C2-9r or ApoB^{11}/si-sc *vs* siα-syn. In contrast and compared to non-tg, the α-syn tg mice treated with C2-9r or ApoB^{11}/si-sc (Fig. 8A, panels in 3d and 5th rows) displayed a 30–35% reduction on TH fibers in the striatum (Fig. 8A, B) and no loss of TH positive fibers in the *S. Nigra* (Fig. 8A, C) as previously reported (Amschl et al., 2013; Spencer et al., 2014a). Treatment of α-syn tg mice with the C2-9r or ApoB^{11}/siα-syn prevented the loss of TH fibers in the striatum to levels resulting in levels comparable to non-tg mice (Fig. 8A, B).

Since accumulation of α-syn in neurons and glial cells in associated with neuro-inflammatory responses that might play a role in neurodegeneration, we next investigated if reducing α-syn had effects on astrogliosis and microgliosis utilizing antibodies against GFAP (Fig. 9)

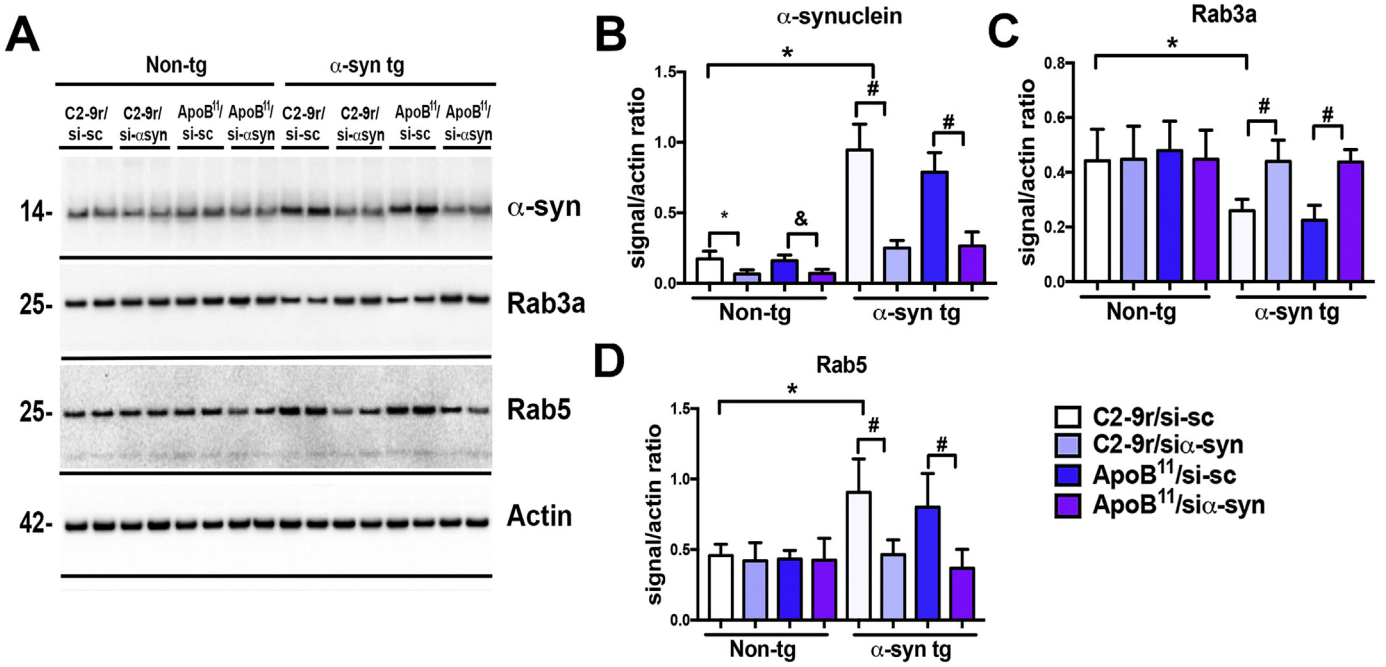

Fig. 6. Immunoblot analysis of the effects of systemic delivery of the siα-syn conjugated to C2-9r or ApoB^{11} peptides of α-syn and endosomal markers in α-syn tg mice. Total homogenates from the cortex were fractioned by ultracentrifugation, the membrane fraction was run for immunoblot analysis. (A) Representative, immunoblot with brain homogenates from non-tg and α-syn tg mice treated with scrambled siRNA (sc-si) or α-syn siRNA (si-αsyn) conjugated to either C2-9r or ApoB^{11} probed with antibodies against α-syn, endosomal markers (Rab3a, Rab5) and ß-actin. Image analysis of levels of immunoreactivity for the bands corresponding to (B) α-syn (14 kDa), (C) Rab3a (26 kDa) and (D) Rab5 (24 kDa) analyzed as ratio to ß-actin signal. One-way ANOVA with poshoc Dunnet when comparing to control and Tukey-Kramer when comparing among groups. Statistical significance $p < 0.05$ compared to: * C2-9r/si-sc non-tg; $^{\&}$ ApoB^{11}/si-sc non-tg; $^{\#}$ ApoB^{11}/si-sc α-syn tg mice. Non-tg (n = 16) and α-syn tg (n = 24).

and Iba1 (Fig. 10) respectively. As previously described with the GFAP antibody, when comparing non-tg mice treated with C2-9r or ApoB^{11}/siα-syn or si-sc, the α-syn tg mice treated with C2-9r or ApoB^{11}/si-sc displayed moderate astrogliosis in the neocortex and hippocampus but not in the striatum (Fig. 9). Whereas, treatment of α-syn tg mice with the C2-9r or ApoB^{11}/siα-syn reduced the astrogliosis both in the neocortex (Fig. 9A, B) and hippocampus (Fig. 9A, C) to levels comparable to non-tg mice (Fig. 9A–D). Similarly, with the Iba1 antibody when comparing to non-tg mice, the α-syn tg mice displayed mild microgliosis in the neocortex and hippocampus but not in the striatum. In contrast, treatment of α-syn tg mice with the C2-9r or ApoB^{11}/siα-syn reduced the microgliosis in the neocortex (Fig. 10A, B) and to a lesser extent in the hippocampus (Fig. 10A, C) to levels comparable to non-tg mice (Fig. 10A–D).

Taken together, these results support the possibility that systemic delivery of oligonucleotides targeting α-syn using either ApoB^{11} or C2-9r ameliorate neurodegenerative and neuroinflammatory pathology associated with α-syn accumulation in a mouse model of PD/DLB.

3. Discussion

Synucleinopathies of the aging population includes DLB, PD and MSA affect over 1.5 million people in the US alone (Alafuzoff and Hartikainen, 2017). Currently no disease modifying therapies are available, but it has been proposed that since α-syn progressively accumulates and triggers toxicity in these disorders that either reducing α-syn synthesis or promoting clearance might be of therapeutic value (Kulisevsky et al., 2018; Valera and Masliah, 2016). In this study, we showed that the 11-amino acid peptide derived from the apolipoprotein B fused with a 9-amino acid Arginine tail (ApoB^{11}) could bind to and transport an siα-syn across the BBB for delivery to neurons and astrocytes following intraperitoneal delivery. Similar to C2-9r, systemically delivered ApoB^{11}/siα-syn effectively reduced α-syn accumulation and ameliorated neurodegeneration and reduced neuro-inflammation in a tg model of synucleinopathy.

These results agree with a previous study showing that knocking down α-syn with systemically administered C2-9r/siα-syn is neuroprotective in a toxic model of PD involving MPTP challenge (Javed et al., 2016). This is consistent with other studies showing that α-syn knock out mice are resistant to MPTP (Dauer et al., 2002; Drolet et al., 2004; Robertson et al., 2004; Tai et al., 2014), 3-nitro propionic acid (Ubhi et al., 2010) and other neurotoxins and that in the α-syn knock out background the neurotoxic effects of APP/Aß are attenuated in tg mice (Spencer et al., 2016a). This new study is different in that instead of using a toxic model of PD we utilized an α-syn tg model (line D) (Masliah et al., 2000; Rockenstein et al., 2002) that is widely used in the field and has been shown to mimic some aspects of PD/DLB. Moreover, in addition to testing C2-9r we investigated the potential value of a novel peptide vector for the delivery of the siα-syn, namely ApoB^{11}. We chose to use this peptide because in earlier studies, we found that the parent peptide ApoB^{38} was highly active at delivering proteins into the CNS (Spencer et al., 2014a; Spencer et al., 2011; Spencer et al., 2016c; Spencer et al., 2015; Spencer et al., 2014b; Spencer and Verma, 2007) and to have an alternative vector to C2-9r. Overall, it was found that both peptides carrying the siα-syn behave similarly, although with ApoB^{11} we observed a more extensive localization to neurons (Fig. 4A–C).

Another difference we observed between the two peptides was the ratio of peptide to siRNA required for complete binding of the oligonucleotide. Previous work from Javed showed an optimal ratio of 40:1 of the C2-9r to siRNA while we showed a ratio of 10:1 for the ApoB^{11} to siRNA (Javed et al., 2016). It is not clear why 4 times less ApoB^{11} peptide is required for complete binding of the same oligonucleotide, although the ApoB^{11} peptide is significantly more hydrophilic than the C2 peptide. A more optimal ratio could be identified by performing subdilutions between the 1:1 and 1:10 that we performed in this experiment to identify a molar ratio of ApoB^{11} that requires less peptide and would maybe reduce the amount of unbound peptide in the injection.

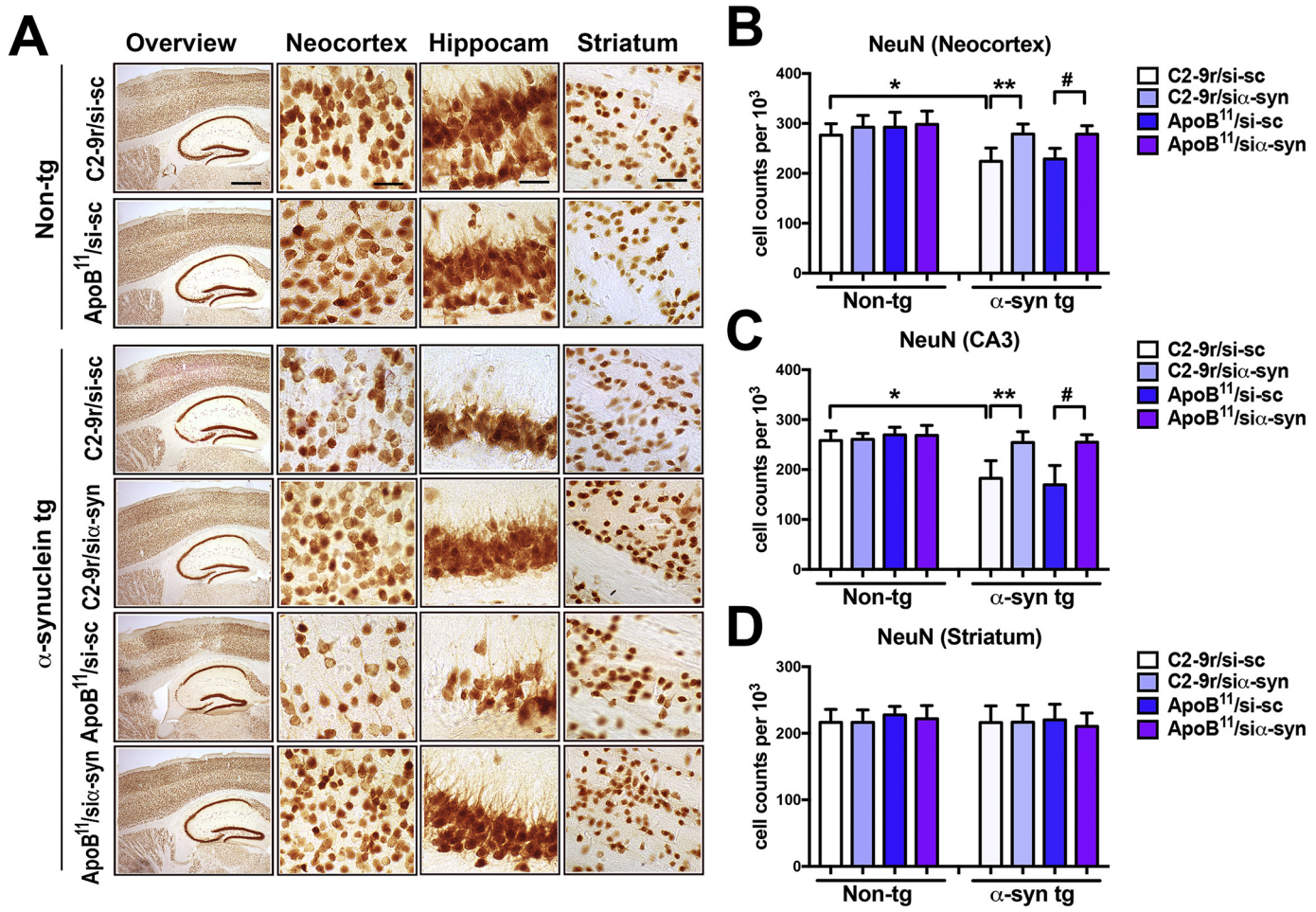

Fig. 7. Immunocytochemical analysis of the effects of systemic delivery of the siα-syn conjugated to C2-9r or ApoB^{11} peptides on total neurons in the brain of α-syn tg mice. Four-month-old α-syn tg and non-tg mice received repeated intraperitoneal injections of scrambled siRNA (si-sc) or α-syn siRNA (si-αsyn) conjugated with either C2-9r or ApoB^{11} and were sacrificed 4 weeks later for analysis. Sections were immunolabeled with an antibody against the neuronal marker NeuN and analyzed by bright field microscopy and stereology (dissector method). (A) Representative images from the neocortex, hippocampus and striatum of non-tg and α-syn tg mice treated with either si-sc or si-αsyn conjugated with C2-9r or ApoB^{11}. Stereological estimates of total NeuN-positive neuronal counts in the hemibrain in the (B) neocortex, (C) hippocampus (CA3), and (D) striatum. One-way ANOVA with poshoc Dunnet when comparing to control and Tukey-Kramer when comparing in between groups. Statistical significance $p < 0.05$ compared to: * non-tg mice; ** C2-9r/si-sc α-*syn*-tg mice; # ApoB^{11}/si-sc α-syn-tg mice. Scale bar represents 250 μm for low magnification panels and 25 μm for higher magnification panels. Non-tg (n = 16) and α-syn tg (n = 24).

Systemic delivery of peptides conjugated to siRNA may necessarily result in distribution to peripheral organs in addition to distribution to the CNS. In fact, we have previously shown that delivery of proteins and enzymes fused to the larger ApoB^{38} peptide are not only widely distributed across the whole CNS, but also to the liver, spleen and muscle (tissues with LDL-R expression) (Spencer et al., 2011; Spencer et al., 2014b; Spencer and Verma, 2007). Although we didn't examine the uptake of siRNA in tissues other than the CNS in this study, we would expect a significant portion of peptide uptake to occur through the liver based on previous work (Spencer et al., 2016d). Delivery of siRNA against α-synuclein to the liver would not necessarily be detrimental as α-syn is specifically expressed in neurons; however, caution would have to be exercised when delivering siRNA against other, more ubiquitous, genes.

Recent evidence suggests that silencing α-synuclein in the adult rat brain may have some detrimental effects (Benskey et al., 2018). Bensksy et al. showed delivery of an shRNA with the AAV vector directly to the *S. Nigra* resulted in loss of TH positive cells as well as increased microglia inflammation (Benskey et al., 2018). Previous work has shown that knockout of α-syn in the mouse has little to no detrimental effect so the knockdown in the adult animal may represent a previously unrealized pathology associated with complete knockdown of α-syn in dopaminergic cells (Abeliovich et al., 2000; Cabin et al., 2002; Dauer et al., 2002; Schluter et al., 2003). Our work *in vitro* and *in vivo* shows only approximately a 50% knockdown of the endogenous mouse α-syn. In addition, we examined the inflammation and levels of TH immunoreactivity in the striatum and the *S. Nigra* and saw no loss of fiber staining in either area when si-αsyn was delivered by either C2-9r or ApoB^{11}. Thus, it is possible that the remaining α-syn is sufficient to prevent the neuronal death and subsequent inflammation observed by Benskey et al.

Earlier studies have shown that direct delivery into the nervous system of nucleotides targeting α-syn can reduce expression levels by 90% (Bourdenx et al., 2014). For example, si and shRNA targeting α-syn have been transferred into the brain of wildtype mice challenged with MPTP or in tg mice (Takahashi et al., 2015) using viral vectors (Sapru et al., 2006) or naked nucleotides (Lewis et al., 2008). Moreover, administration of naked mir-7 and mir-153 (Doxakis, 2010) or AAV delivered mir-30 has been shown to silence α-syn (Khodr et al., 2014). We have shown that delivery of a lentivirus expressing mir-101 reduces α-syn accumulation in the brains of a tg model of MSA (Valera et al., 2017). In contrast to this research where α-syn expression was abrogated by direct delivery of nucleotides into the CNS, for this study we explored the use of small peptide vectors for systemic delivery. The

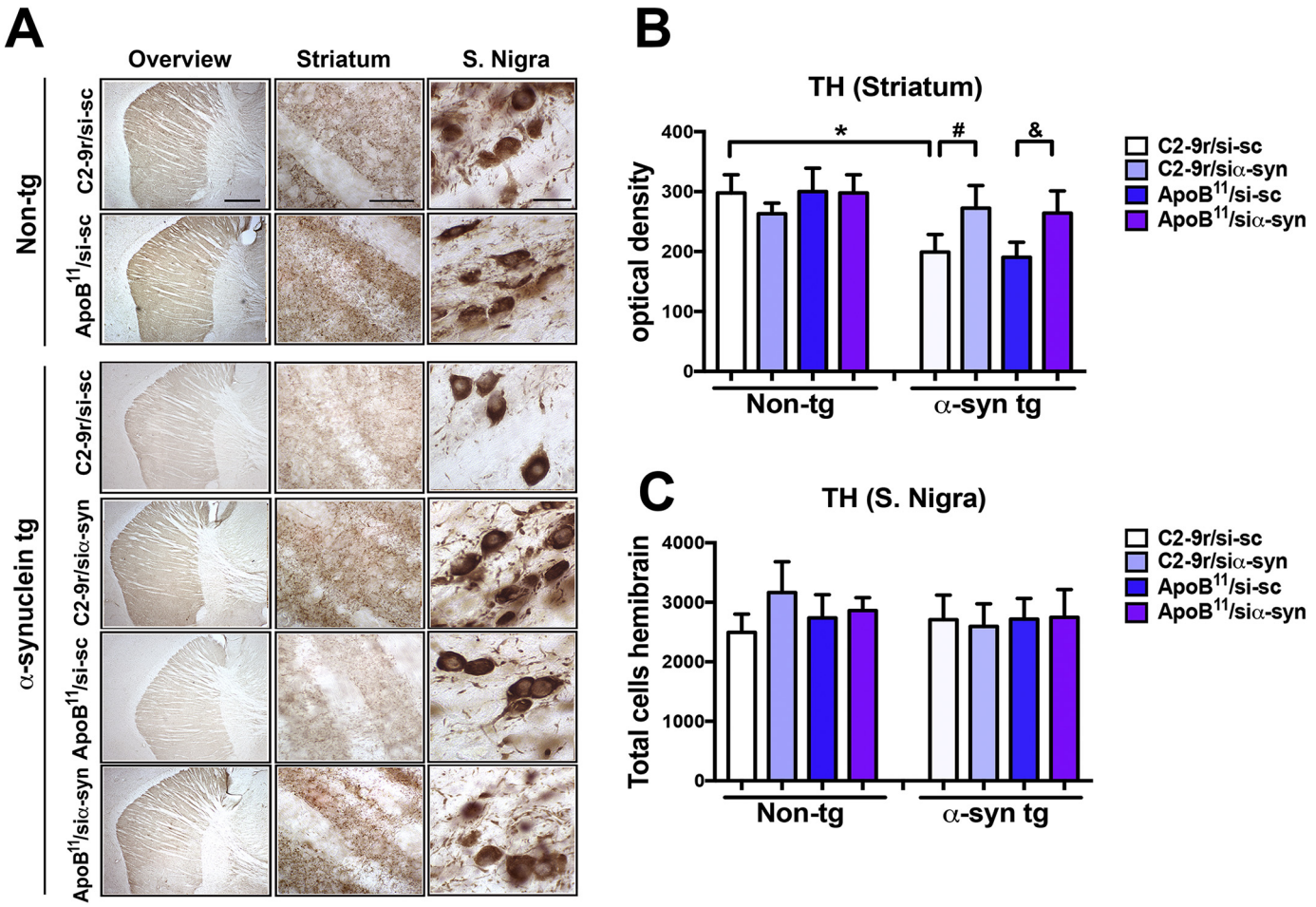

Fig. 8. Immunocytochemical analysis of the effects of systemic delivery of the siα-syn conjugated to C2-9r or ApoB^{11} peptides on tyrosine hydroxylase dopaminergic neurons and terminals in the brain of α-syn tg mice. Four-month-old α-syn tg and non-tg mice received repeated intraperitoneal injections of scrambled siRNA (si-sc) or α-syn siRNA (si-αsyn) conjugated to either C2-9r, ApoB^{11} and were sacrificed 4 weeks later for analysis. Sections were immunolabeled with an antibody against the dopaminergic neuronal marker tyrosine hydroxylase (TH) and analyzed by bright field microscopy for optical density (striatum) and stereology (*S. Nigra* pars compacta, dissector method). (A) Representative images of TH immunostaining in the striatum and *S. Nigra* of non-tg and α-syn tg mice treated with either si-sc or si-αsyn conjugated with C2-9r or ApoB^{11}. (B) Optical density analysis of TH positive fibers in the striatum. (C) Stereological analysis estimates (hemibrain) of numbers of TH positive neurons in the *S. Nigra*. One-way ANOVA with poshoc Dunnet when comparing to control and Tukey-Kramer when comparing in between groups. Statistical significance $p < 0.05$ compared to: * non-tg mice; ** C2-9r/si-sc α-syn-tg mice; $^{\&}$ ApoB^{11}/si-sc α-syn-tg mice. Scale bar represents 250 μm for low magnification panels and 25 μm for higher magnification panels. Non-tg (n = 16) and α-syn tg (n = 24).

ApoB^{11} peptide could be used to deliver any form or design of nucleotides including, but not limited to: cDNA, mRNA, siRNA, shRNA, miRNA, gRNA or synthetic nucleotide sequences. Systemic delivery of oligonucleotides to the CNS could be beneficial for neurodegenerative diseases, neuro-modulatory treatments, cancers of the CNS, gene targeted editing of the CNS or anti-microbial gene delivery of the CNS.

As shown here, systemic delivery of siRNA by either the ApoB^{11} or C2-9r peptide (Javed et al., 2016) to the CNS occurred primarily to neurons and only to a lesser extent the astrocytes as measured by co-labeling studies with NeuN and GFAP respectively. We previously showed with the larger ApoB^{38} peptide fused to the protease, neurosin, that uptake occurred primarily with neurons and to a lesser extent astrocytes, microglia and oligodendrocytes (Spencer et al., 2015). This pattern closely resembled the pattern of LDL-R expression levels on these cells as the peptide relies on this receptor for endocytosis into the cell (Spencer et al., 2015). Following endocytosis, the siRNA must escape the endosome as a naked oligonucleotide to function as an inhibitor molecule. The process of this escape mechanism is unclear; however, previous studies have shown other proteins and antibodies have escaped the endosome following endocytosis with the ApoB^{38} peptide suggesting a mechanism must exist (Spencer et al., 2014a; Spencer et al., 2011; Spencer et al., 2016c; Spencer et al., 2015; Spencer and Verma, 2007). It is possible that binding to HDL or LDL molecules through the ApoB peptide may facilitate escape of the endosome *via* SR-BI receptor, thus bypassing the lysosome fusion (Lim et al., 2013; Wolfrum et al., 2007). This would allow escape of the peptide:RNA complex to the cytoplasm where it could access the mRNA for RISC mediated endonuclease digestion (Hammond, 2005).

The Apolipoprotein B protein binds to the LDL receptor at the surface of the endothelial cells on the BBB inducing endocytosis and transytosis to the CNS side where it is released for binding to receptors on neurons and astrocytes. Similarly, we believe the ApoB^{11} peptide binds to the LDL-R and transports siRNA to the CNS. In contrast, the RGD peptide binds to the nicotinic acetylcholine receptor (nAch) (Lentz, 1991) on neurons for uptake, although the receptor used for binding and transport across the blood-brain barrier is not known, as nAch and other known RGD binding receptors are not expressed on BBB endothelial model cells such as bEnd.3 or BCECs (Tian et al., 2015). However, other atypical nAch α-subunits have been detected by RT-PCR in rat arterial endothelial cells possibly explaining the uptake and transport mechanism at the BBB (Bruggmann et al., 2002; Bruggmann et al., 2003). These alternate receptors may also be responsible for the

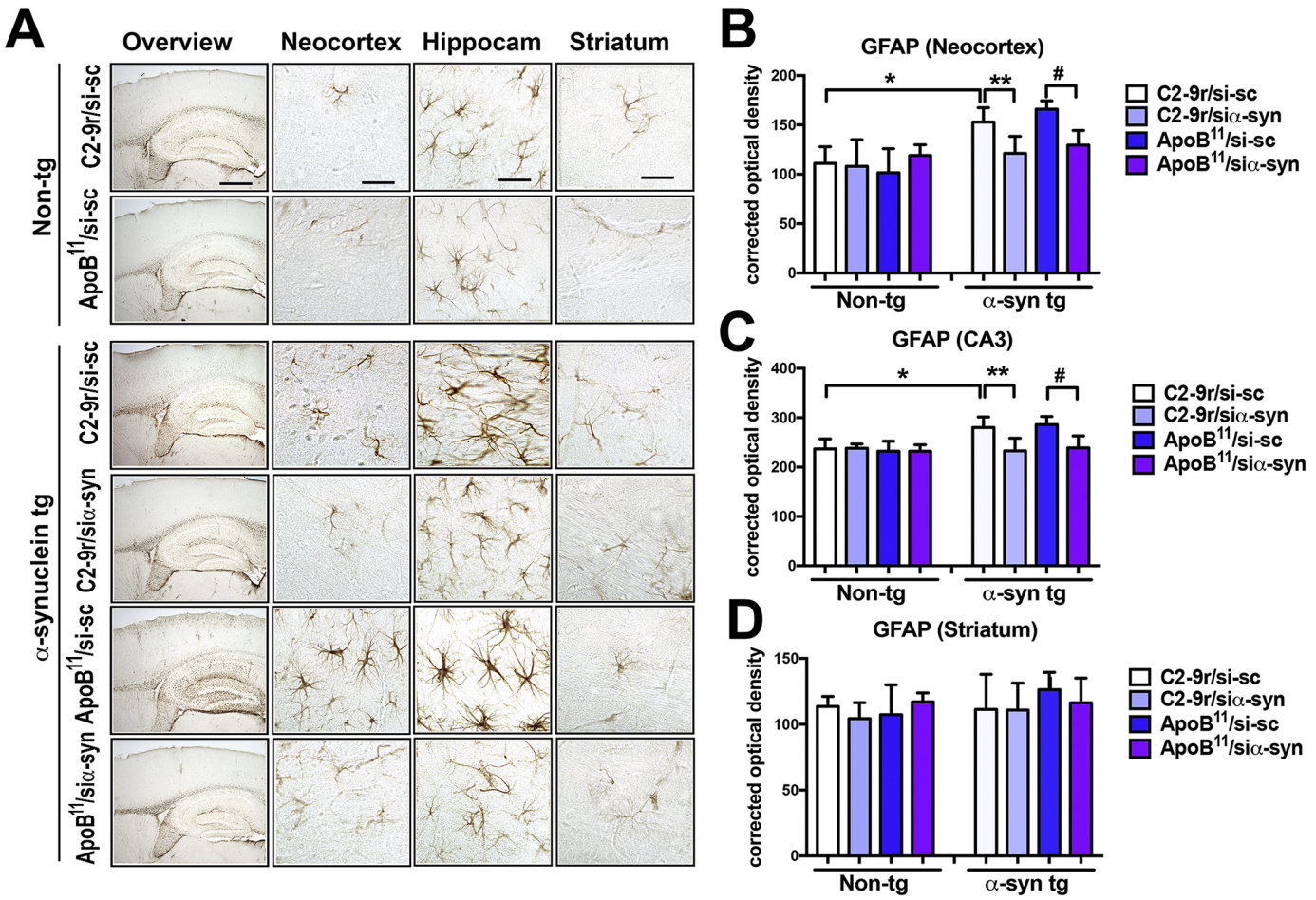

Fig. 9. Immunocytochemical analysis of the effects of systemic delivery of the siα-syn conjugated to C2-9r or ApoB^{11} peptides on astrogliosis in the brains of α-syn tg mice. Four-month-old α-syn tg and non-tg mice received repeated intraperitoneal injections of scrambled siRNA (si-sc) or α-syn siRNA (si-αsyn) conjugated to either C2-9r or ApoB^{11} and were sacrificed 4 weeks later for analysis. Sections were immunolabeled with an antibody against the astroglial cell marker glial fibrillary acidic protein (GFAP). (A) Representative images of the patters of GFAP immunoreactivity in the neocortex, hippocampus and striatum of non-tg and α-syn tg mice treated with either si-sc or si-αsyn conjugated with C2-9r or ApoB^{11}. Image analysis of levels of GFAP immunoreactivity expressed as corrected optical density in the (B) neocortex, (C) hippocampus (CA3), and (D) striatum. One-way ANOVA with poshoc Dunnet when comparing to control and Tukey-Kramer when comparing in between groups. * indicates statistical significance $p < 0.05$ compared to non-tg mice. ** $p < 0.05$ compared to C2-9r/si-sc. # indicates statistical significance $p < 0.05$ compared to α-syn-tg mice treated with ApoB^{11}/si-sc. Scale bar represents 250 μm for low magnification panels and 25 μm for higher magnification panels. Non-tg (n = 16) and α-syn tg (n = 24).

uptake by astrocytes. In fact, the α7 nAchR has been detected in cultured neonatal rat microglial cells (Suzuki et al., 2006). Recent studies have shown an upregulation of nAchR in the caudate nucleus of Parkinson's patients with a concomitant downregulation in the putamen, thus potentially complicating the targeting of the C2-9r directed siRNA for Parkinson's disease (Isaias et al., 2014). It remains to be seen what role each of these peptides may play in therapeutic interventions for different targets.

Although the $t_{1/2}$ of the siRNA wasn't examined in this study, previous studies have shown the half-life of unprotected RNA in the serum to be approximately 2 h (Javed et al., 2016; Layzer et al., 2004) and in the rodent following intravenous delivery of 6 min (Soutschek et al., 2004). Once inside the cell, the siRNA has a long half-life and has shown knockdown of the target gene for as long as 3 days in dividing cells and 3–4 weeks in non-dividing cells (Bartlett and Davis, 2006; Layzer et al., 2004). In order to increase the effectiveness and therapeutic potential of siRNAs for CNS delivery, longer $t_{1/2}$ in the serum would be beneficial. Introduction of 2′-fluoro or 2′-O'methyl sugar modifications function to increase endonuclease resistance and stabilizing siRNA duplexes. In fact, 2′-F modified siRNAs have an increased serum $t_{1/2}$ of approximately 24 h (Layzer et al., 2004). Currently, 2′-F modified siRNAs are approved for clinical use (Fomivirsen and Macugen) (Stein and Castanotto, 2017). Other modifications that could be considered include morpholinos, peptide nucleic acids and phosphorthioate sugars (Wang et al., 2017).

Since the transport with receptors targeted for transport across the BBB are saturable (Duffy et al., 1988; Wunner et al., 1984), identification of multiple methods of transport may be necessary for the delivery of more than one therapy simultaneously. Starzyk et al. showed that the transferrin receptor could be used for transport of proteins across the BBB (Friden et al., 1991) and subsequently, the IGF-R was used to transport proteins (Coloma et al., 2000; Pardridge et al., 1995). These receptors work similarly to the LDLR family of receptors in that they (a) bind protein on the basal/ blood side, (b) transport by transytosis to the neuronal side, and (c) release the protein on the neuronal side of the BBB (Bickel et al., 2001). Targeting different receptor pathways for different therapeutics will prevent the possibility of overwhelming the transport kinetics at the BBB thus allowing simultaneous delivery of multiple therapeutic options. It remains to be seen if the 11-amino acid ApoB peptide can function to transport larger proteins with the same efficiency as the previously published 38 amino acid ApoB^{38} peptide. Additional studies will be needed to determine these kinetics as well as how long lasting are the neuroprotective effects of α-syn knocked down with these two small peptide vectors. Moreover,

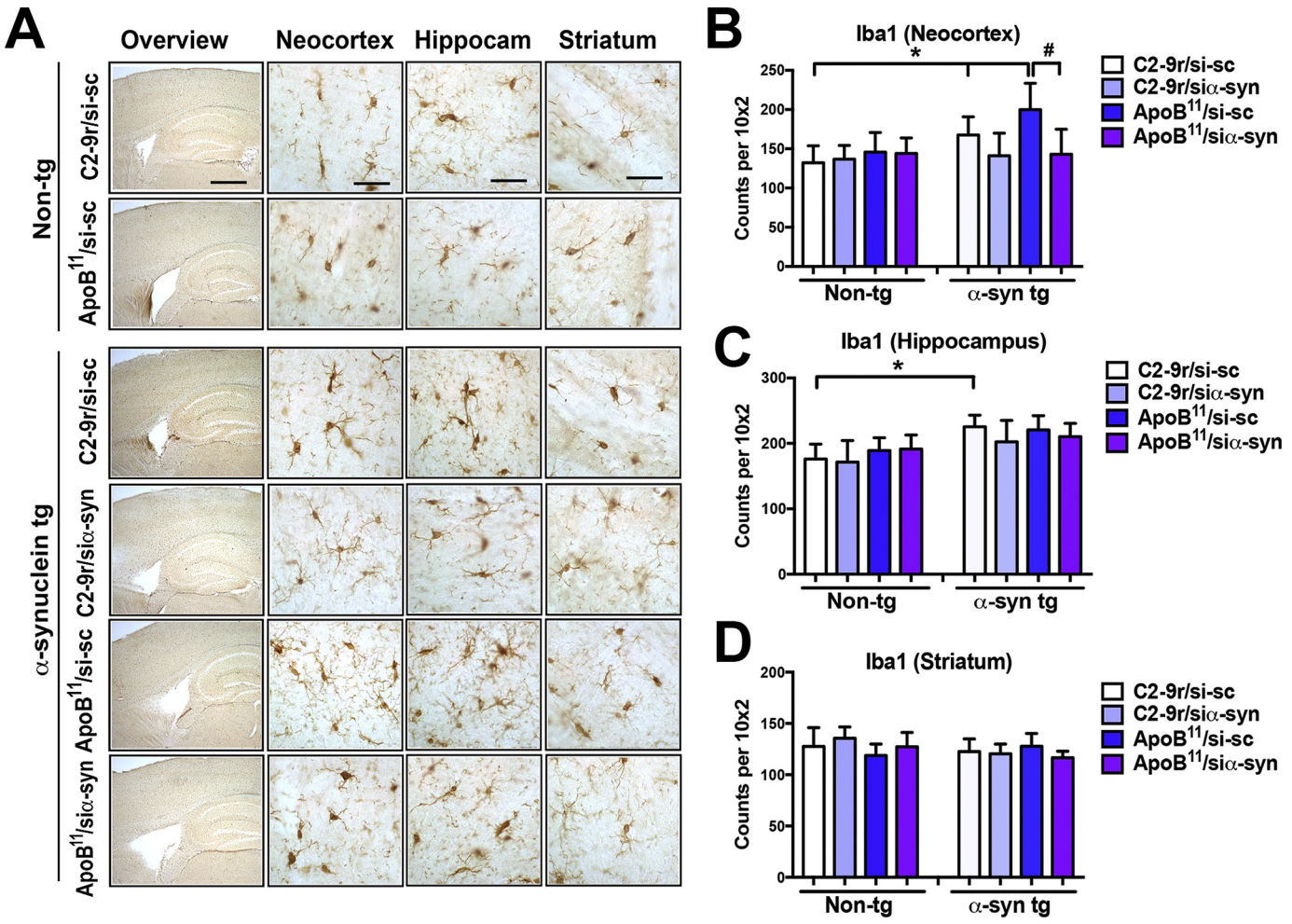

Fig. 10. Immunocytochemical analysis of the effects of systemic delivery of the siα-syn conjugated to C2-9r or ApoB^{11} peptides on microgliosis in the brains of α-syn tg mice. Four-month-old α-syn tg and non-tg mice received repeated intraperitoneal injections of scrambled siRNA (si-sc) or α-syn siRNA (si-αsyn) conjugated to either C2-9r or ApoB^{11} and were sacrificed 4 weeks later for analysis. Sections were immunolabeled with an antibody against the microglia cell marker- Iba1. (A) Representative images of the neocortex, hippocampus and striatum of non-tg and α-syn tg mice treated with either si-sc or si-αsyn conjugated with C2-9r or ApoB^{11} of sections immunostained with the Iba1 antibody. Image analysis of the relative numbers of Iba1 immunoreactive cells per 10^2 in the (B) neocortex, (C) hippocampus (CA3), and (D) striatum. One-way ANOVA with poshoc Dunnet when comparing to control and Tukey-Kramer when comparing in between groups. * indicates statistical significance $p < 0.05$ compared to non-tg mice. **$p < 0.05$ compared to C2-9r/si-sc. # indicates statistical significance $p < 0.05$ compared to α-syn-tg mice treated with ApoB^{11}/si-sc. Scale bar represents 250 μm for low magnification panels and 25 μm for higher magnification panels. Non-tg (n = 16) and α-syn tg (n = 24).

detailed behavioral and functional analysis will be needed to further evaluate the potential therapeutic value of this approach in synucleinopathies.

In summary, we have identified a 11-amino acid LDL-R binding peptide that can transport siα-syn across the BBB as a therapeutic option for synucleinopathies such as PD and DLB. The ApoB^{11} peptide, along with the C2-9r peptide, represent two potential approaches for the delivery of siRNAs or other oligonucleotides to the CNS for therapies.

4. Methods and experimental design

4.1. Preparation of peptide vectors and siRNAs

For this study we utilized two peptide vectors to deliver the siRNA targeting α-syn. The first was a validated (as positive control) peptide namely C2-9r, (NH_2CDIFTNSRGKRAGGGGrrrrrrrrr) that was developed by the addition of four Gly (G) and nine d-Arg (9r) residues to the C-terminus of the C2 peptide, derived from a 29 residue rhabdovirus glycoprotein and has been previously described (Javed et al., 2016). The second and novel vector was the ApoB^{11}, a smaller peptide linked to a 9r (NH_2RLTRKRGLKLAGGGGGRRRRRRRRR) derived from the ApoB^{38} peptide that we have previously shown to effectively transport antibodies, proteases and trophic factors across the BBB (Spencer et al., 2014a; Spencer et al., 2011; Spencer et al., 2016c; Spencer et al., 2015; Spencer et al., 2014b; Spencer and Verma, 2007). The peptide was synthesized to 90% purity by Karebay Biochem, Inc.

Peptides were diluted to 10 mM in PBS (Life Technologies). The siα-syn (5'GAC UUU CAA AGG CCA AGG A) corresponding to nucleotides 168–186 of α-synuclein was chosen because we have previously shown targets both mouse and human α-syn (Spencer et al., 2016a). As control we used an si-scrambled (5'GGG CAU ACU GAG CUA ACA A). The siRNAs were purchased from ValueGene, Inc. and desalted. For *in vitro* and *in vivo* trafficking experiments a FITC labeled si-αsyn RNA labeled at 5′ was utilized and prepared. Oligonucleotides were re-suspended in RNAse free water (Life Technologies) at 100 mM and aliquoted. The siRNA's (si-sc and siα-syn) and peptide's (ApoB^{11} and C2-9r) were mixed at specified ratios in PBS (1:0, 0:1, 1;1, 1:10, 1:20, 1:40, 1:60) and incubated at room temperature for 30 min to allow RNA to bind to peptide.

5. Neuronal cell lines, treatments and analysis

The mouse cholinergic cell line Neuro2A (N2A) was utilized for *in vitro* experiments (Kojima et al., 1994). N2A cells were plated at 1×10^5 cells/well of a 12 well dish on poly L-lysine coated glass coverslips in DMEM +1% FBS for 5 days to allow for differentiation (Spencer et al., 2016a). Cells were treated with 100 pmol siRNA (FITC tagged): peptide for 0, 3, 24 and 48 h and then fixed in 4% paraformaldehyde. Immunolabeling was performed as previously described (Spencer et al., 2016b) with an antibody against MAP2 (Mouse monoclonal, Millipore, 1:5000) detected with Tyramide Red system (NEN Life Sciences) and analysis of uptake of the FITC labeled siRNA was performed by laser scanning confocal microscopy (BioRad, MRC1024) (Spencer et al., 2016a).

Additional experiments included treating N2A cells with untagged siRNA (100 pmol): peptide for 0, 24, 48 and 72 h. Control experiments were performed by treating a mouse cell line with the si-sc/peptide and the siα-syn/peptide for 24 h. Then cells in coverslips were double immunolabeled with antibodies against MAP2 (1:200, Millipore) and α-syn (Syn-1, mouse monoclonal, 1:5000, BD Biosciences), α-syn was detected with the Tyramide Red system (NEN Life Sciences) whereas MAP2 was detected with FITC-tagged antibodies (1:75; Vector). Coverslips were imaged with a Zeiss 63 × 1.4 objective on an Axiovert 35 microscope (Zeiss) with an attached MRC1024 laser scanning confocal microscope (LSCM) system (BioRad) and analyzed with Image J to determine pixel intensity (Spencer et al., 2016a).

6. Animal care and tissue processing

All experiments described were carried out in strict accordance with good animal practice according to NIH recommendations, and all procedures for animal use were approved by the Institutional Animal Care and Use Committee at the University of California at San Diego (UCSD) under protocol #S07221. At the end of the 30-day treatment, the mice were sacrificed and the right hemibrains were snap-frozen and stored at −70 °C for biochemical analysis, while the left hemibrains were fixed 4% paraformaldehyde for vibratome sectioning (40 μm) and neuropathological analysis.

7. Transgenic mouse lines and treatments

For this study, mice over-expressing α-syn from the platelet-derived growth factor β (PDGF-β) promoter (Line D) were utilized (Masliah et al., 2000; Rockenstein et al., 2002). This model was selected because mice from this line develop intraneuronal α-synuclein aggregates distributed through the neocortex and hippocampus similar to what has been described in LBD. Moreover, expression levels of the transgene are moderate (0.5–1.0 fold over baseline) allowing more clear analysis of the effects of the siRNA and these animals display loss of dopaminergic fibers in the striatum and mild motoric deficits. At first, we compared trafficking and distribution of the siRNA following intra-venous *vs* intra-peritoneal injection. For this purpose, non-tg mice (total, $n = 18$) received a single intra-venous ($n = 9$) or intra-peritoneal (n = 9) injection of 50 μg of 5' FITC naked siα-syn ($n = 3$), C9-2r/siα-syn (n = 3) or ApoB^{11}/ siα-syn (n = 3) and 4 h later were terminated for analysis. Then, to study the trafficking and anatomical and cellular location of the siRNA, non-tg ($n = 12$) and α-syn tg (total n = 12) received a single intra-peritoneal injection of 50 μg of 5′ FITC labeled naked siα-syn (n = 3 per genotype) or siα-syn conjugated to either C2-9r (n = 3, per genotype/group) or ApoB^{11} (n = 3), per genotype/group) and 4 h later were sacrificed.

To determine the ability of the systemically administered siRNA/protein conjugate to ameliorate neurodegeneration and α-syn pathology groups of non-tg ($n = 16$; 4 m/o) and α-syn tg ($n = 24$; 4 m/o) mice received intra-peritoneal injections of 50 μg of C2-9r/ si-sc ($n = 4$ per group non-tg and $n = 6$ per group α-syn tg); ApoB^{11}/si-sc (n = 4 per group non-tg and n = 6 per group α-syn tg); C9-2r/siα-syn (n = 4 per group non-tg and n = 6 per group α-syn tg)or ApoB^{11}/ siα-syn (n = 4 per group non-tg and n = 6 per group α-syn tg) twice weekly for four weeks. Following NIH guidelines for the humane treatment of animals, mice were anesthetized with chloral hydrate and flush-perfused transcardially with 0.9% saline. Brains and peripheral tissues were removed and divided sagitally. The right hemibrain was post-fixed in phosphate-buffered 4% PFA (pH 7.4) at 4 °C for 48 h for neuropathological analysis, while the left hemibrain was snap-frozen and stored at −70 °C for subsequent protein analysis.

8. Immunoblot analysis

Cell lysates and mouse hemibrains were homogenized as previously described (Crews et al., 2010; Spencer et al., 2009). For immunoblot analysis, 20 μg of total protein per lane was loaded on 4–12% Bis-Tris SDS-PAGE gels and blotted onto polyvinylidene fluoride membranes. Membranes were probed with antibodies against total α-syn (Syn-1, BD Biosciences). Incubation with primary antibody was followed by species-appropriate incubation with secondary antibody tagged with horseradish peroxidase (Santa Cruz Biotechnology) and visualization with enhanced chemiluminescence. Analysis of all immunoblot was performed with a Versadoc XL imaging apparatus (BioRad) using β-actin (Sigma) levels as a loading control.

9. Immunocytochemical and neuropathological analyses

Briefly as previously described (Spencer et al., 2016a) blind-coded sagittal brain vibratome sections were treated at 4 °C for overnight with primary antibodies against α-syn (Syn-1, BD Biosciences, mouse monoclonal, 1:500), neuronal marker NeuN (Millipore, mouse monoclonal, 1:1000), dopaminergic marker tyrosine hydroxylase (TH) (Millipore, mouse monoclonal, 1:1000), astroglial marker GFAP (Millipore, mouse monoclonal, 1:1000) and microglial cell marker Iba-1 (Abcam, goat polyclonal, 1:500) respectively. Following overnight incubation, the sections were incubated with biotinylated-secondary antibodies and detected with avidin D-HRP (ABC Elite, Vector Laboratories, Burlingame, CA). To determine α-syn neuropathology (Syn-1) and astrogliosis (GFAP), the brain sections were imaged by Olympus BX41microscope. The levels of immunoreactivity were determined by optical density analysis using Image Quant 1.43 program (NIH). From each section a total of 10 digital fields 1024 × 1024 pixels in the neocortex and hippocampus were analyzed. Levels of optical density were corrected to background using sections stained in the absence of the primary antibody. The numbers of α-syn inclusion positive cells were determined per field (100 μm^2). To estimate neuronal cell numbers briefly as previously described (Overk et al., 2014), the numbers of NeuN-immunoreactive neurons in the hippocampus were estimated utilizing unbiased stereological methods. The CA3 region of the hippocampus was outlined using an Olympus BX51 microscope running Stereo-Investigator 8.21.1 software (Micro-BrightField, Cochester, VT) (grid sizes 150 × 150 μm and the counting frames were 30 × 30 μm). The average coefficient of error for each region was below 0.1. Sections were analyzed using a 100 × 1.4 PlanApo oil-immersion objective. The average mounted tissue thickness allowed for 2 μm top and bottom guard-zones and a 5 μm high dissector. Similarly, the number of TH (*S. Nigra*) immunoreactive neurons were estimated using unbiased stereological methods (Overk et al., 2014). In addition, the density of TH positive axonal fibers in the striatum was analyzed by optical density as described above. To analyze microglial cell morphology briefly as previously described (El-Agnaf et al., 2017), sections labeled with Iba-1 were analyzed utilizing the Image-Pro Plus program (Media Cybernetics, Silver Spring, MD) (10 digital images 1024 × 1024 pixels per section) and analyzed in order to estimate the average number of microglial cells per unit area (100 μm^2) and ramifications of Iba-1 positive microglia (Morrison and Filosa, 2013).

To determine the distribution and cellular localization of the naked or C2-9r or ApoB[11] FITC tagged siRNA, co-labeling experiments were performed as previously described (Spencer et al., 2013). For this purpose, vibratome sections were immunolabeled with antibodies against α-syn (Syn-1, BD Biosciences, mouse monoclonal, 1:5000), NeuN (Millipore, mouse monoclonal, 1:10,000) and GFAP (Millipore, mouse monoclonal, 1:10,000) followed by detection with the Tyramide Signal Amplification™-Direct (Red) system (NEN Life Sciences) while the siRNA was directly visualized by the appended FITC label. Sections were imaged with a Zeiss 63× (N.A. 1.4) objective on an Axiovert 35 microscope (Zeiss) with an attached MRC1024 LSCM system (BioRad) (Masliah et al., 2000).

9.1. Statistical analysis

All experiments were performed blind coded and in triplicate. Values in the figures are expressed as means ± SEM. To determine the statistical significance, values were compared by using the one-way ANOVA with posthoc Dunnet when comparing the non-tg controls *vs* α-syn tg mice. Additional comparisons among groups treated with C2-9r or ApoB[11]/siα-syn or si-sc were done using Tukey-Krammer or Fisher posthoc tests. The differences were considered to be significant if p values were < 0.05.

Acknowledgements

Supported by NIH grants AG05131 and AG18440.

References

Abbott, N.J., et al., 2006. Astrocyte-endothelial interactions at the blood-brain barrier. Nat. Rev. Neurosci. 7, 41–53.
Abeliovich, A., et al., 2000. Mice lacking alpha-synuclein display functional deficits in the nigrostriatal dopamine system. Neuron 25, 239–252.
Alafuzoff, I., Hartikainen, P., 2017. Alpha-synucleinopathies. Handb. Clin. Neurol. 145, 339–353.
Alarcon-Aris, D., et al., 2018. Selective alpha-synuclein knockdown in monoamine neurons by intranasal oligonucleotide delivery: potential therapy for Parkinson's disease. Mol. Ther. 26, 550–567.
Alves, S., et al., 2016. Gene therapy strategies for Alzheimer's disease: an overview. Hum. Gene Ther. 27, 100–107.
Amschl, D., et al., 2013. Time course and progression of wild type alpha-synuclein accumulation in a transgenic mouse model. BMC Neurosci. 14, 6.
Bartlett, D.W., Davis, M.E., 2006. Insights into the kinetics of siRNA-mediated gene silencing from live-cell and live-animal bioluminescent imaging. Nucleic Acids Res. 34, 322–333.
Begley, D.J., 2004. ABC transporters and the blood-brain barrier. Curr. Pharm. Des. 10, 1295–1312.
Begley, D.J., Brightman, M.W., 2003. Structural and functional aspects of the blood-brain barrier. Prog. Drug Res. 61, 39–78.
Benskey, M.J., et al., 2018. Silencing alpha synuclein in mature Nigral neurons results in rapid neuroinflammation and subsequent toxicity. Front. Mol. Neurosci. 11, 36.
Bickel, U., et al., 2001. Delivery of peptides and proteins through the blood-brain barrier. Adv. Drug Deliv. Rev. 46, 247–279.
Bourdenx, M., et al., 2014. Down-regulating alpha-synuclein for treating synucleopathies. Mov. Disord. 29, 1463–1465.
Brettschneider, J., et al., 2015. Spreading of pathology in neurodegenerative diseases: a focus on human studies. Nat. Rev. Neurosci. 16, 109–120.
Bruggmann, D., et al., 2002. Multiple nicotinic acetylcholine receptor alpha-subunits are expressed in the arterial system of the rat. Histochem. Cell Biol. 118, 441–447.
Bruggmann, D., et al., 2003. Rat arteries contain multiple nicotinic acetylcholine receptor alpha-subunits. Life Sci. 72, 2095–2099.
Cabin, D.E., et al., 2002. Synaptic vesicle depletion correlates with attenuated synaptic responses to prolonged repetitive stimulation in mice lacking alpha-synuclein. J. Neurosci. 22, 8797–8807.
Cairns, N.J., et al., 2007. Neuropathologic diagnostic and nosologic criteria for frontotemporal lobar degeneration: consensus of the consortium for frontotemporal lobar degeneration. Acta Neuropathol. 114, 5–22.
Chandra, S., et al., 2004. Double-knockout mice for alpha- and beta-synucleins: effect on synaptic functions. Proc. Natl. Acad. Sci. U. S. A. 101, 14966–14971.
Chang, J.L., et al., 2018. Targeting amyloid-beta precursor protein, APP, splicing with antisense oligonucleotides reduces toxic amyloid-beta production. Mol. Ther. 26, 1539–1551.
Coloma, M.J., et al., 2000. Transport across the primate blood-brain barrier of a genetically engineered chimeric monoclonal antibody to the human insulin receptor. Pharm. Res. 17, 266–274.
Crews, L., et al., 2010. Selective molecular alterations in the autophagy pathway in patients with Lewy body disease and in models of alpha-synucleinopathy. PLoS One 5, e9313.
Crunkhorn, S., 2017. Alzheimer disease: antisense oligonucleotide reverses tau pathology. Nat. Rev. Drug Discov. 16, 166.
Dauer, W., et al., 2002. Resistance of alpha -synuclein null mice to the parkinsonian neurotoxin MPTP. Proc. Natl. Acad. Sci. U. S. A. 99, 14524–14529.
De Strooper, B., Karran, E., 2016. The cellular phase of Alzheimer's disease. Cell. 164, 603–615.
DeVos, S.L., Hyman, B.T., 2017. Tau at the crossroads between neurotoxicity and neuroprotection. Neuron. 94, 703–704.
Dickey, A.S., La Spada, A.R., 2018. Therapy development in Huntington disease: from current strategies to emerging opportunities. Am. J. Med. Genet. A 176, 842–861.
Doxakis, E., 2010. Post-transcriptional regulation of alpha-synuclein expression by mir-7 and mir-153. J. Biol. Chem. 285, 12726–12734.
Drolet, R.E., et al., 2004. Mice lacking alpha-synuclein have an attenuated loss of striatal dopamine following prolonged chronic MPTP administration. Neurotoxicology 25, 761–769.
Duffy, K.R., et al., 1988. Human blood-brain barrier insulin-like growth factor receptor. Metabolism 37, 136–140.
El-Agnaf, O., et al., 2017. Differential effects of immunotherapy with antibodies targeting alpha-synuclein oligomers and fibrils in a transgenic model of synucleinopathy. Neurobiol. Dis. 104, 85–96.
Eller, M., Williams, D.R., 2011. alpha-synuclein in Parkinson disease and other neurodegenerative disorders. Clin. Chem. Lab. Med. 49, 403–408.
Fang, F., et al., 2017. Synuclein impairs trafficking and signaling of BDNF in a mouse model of Parkinson's disease. Sci. Rep. 7, 3868.
Friden, P.M., et al., 1991. Anti-transferrin receptor antibody and antibody-drug conjugates cross the blood-brain barrier. Proc. Natl. Acad. Sci. U. S. A. 88, 4771–4775.
Fu, H., et al., 2018. Selective vulnerability in neurodegenerative diseases. Nat. Neurosci. 21, 1350–1358.
Ghosh, R., Tabrizi, S.J., 2017. Gene suppression approaches to neurodegeneration. Alzheimers Res. Ther. 9, 82.
Gibbons, G.S., et al., 2018. Mechanisms of cell-to-cell transmission of pathological tau: a review. JAMA Neurol. 76, 101–108.
Hammond, S.M., 2005. Dicing and slicing: the core machinery of the RNA interference pathway. FEBS Lett. 579, 5822–5829.
Isaias, I.U., et al., 2014. Nicotinic acetylcholine receptor density in cognitively intact subjects at an early stage of Parkinson's disease. Front. Aging Neurosci. 6, 213.
Iwai, A., et al., 1995. The precursor protein of non-A beta component of Alzheimer's disease amyloid is a presynaptic protein of the central nervous system. Neuron 14, 467–475.
Javed, H., et al., 2016. Development of nonviral vectors targeting the brain as a therapeutic approach for Parkinson's disease and other brain disorders. Mol. Ther. 24, 746–758.
Jucker, M., Walker, L.C., 2018. Propagation and spread of pathogenic protein assemblies in neurodegenerative diseases. Nat. Neurosci. 21, 1341–1349.
Kao, S.C., et al., 2004. BACE1 suppression by RNA interference in primary cortical neurons. J. Biol. Chem. 279, 1942–1949.
Keiser, M.S., et al., 2016. Gene suppression strategies for dominantly inherited neurodegenerative diseases: lessons from Huntington's disease and spinocerebellar ataxia. Hum. Mol. Genet. 25, R53–R64.
Khodr, C.E., et al., 2014. Targeting alpha-synuclein with a microRNA-embedded silencing vector in the rat substantia nigra: positive and negative effects. Brain Res. 1550, 47–60.
Knott, T.J., et al., 1986. Complete protein sequence and identification of structural domains of human apolipoprotein B. Nature 323, 734–738.
Kojima, N., et al., 1994. Induction of cholinergic differentiation with neurite sprouting by de novo biosynthesis and expression of GD3 and b-series gangliosides in Neuro2a cells. J. Biol. Chem. 269, 30451–30456.
Koutsilieri, E., et al., 2007. The therapeutic potential of siRNA in gene therapy of neurodegenerative disorders. J. Neural Transm. Suppl. 43–49.
Kulisevsky, J., et al., 2018. Update in therapeutic strategies for Parkinson's disease. Curr. Opin. Neurol. 31, 439–447.
Lajoie, J.M., Shusta, E.V., 2015. Targeting receptor-mediated transport for delivery of biologics across the blood-brain barrier. Annu. Rev. Pharmacol. Toxicol. 55, 613–631.
Lashuel, H.A., et al., 2013. The many faces of alpha-synuclein: from structure and toxicity to therapeutic target. Nat. Rev. Neurosci. 14, 38–48.
Layzer, J.M., et al., 2004. In vivo activity of nuclease-resistant siRNAs. RNA 10, 766–771.
Lee, E.B., et al., 2011a. Gains or losses: molecular mechanisms of TDP43-mediated neurodegeneration. Nat. Rev. Neurosci. 13, 38–50.
Lee, S.J., et al., 2011b. Protein aggregate spreading in neurodegenerative diseases: problems and perspectives. Neurosci. Res. 70, 339–348.
Lentz, T.L., 1991. Structure-function relationships of curaremimetic neurotoxin loop 2 and of a structurally similar segment of rabies virus glycoprotein in their interaction with the nicotinic acetylcholine receptor. Biochemistry 30, 10949–10957.
Lewis, J., et al., 2008. In vivo silencing of alpha-synuclein using naked siRNA. Mol. Neurodegener. 3, 19.
Lim, H.Y., et al., 2013. Lymphatic vessels are essential for the removal of cholesterol from peripheral tissues by SR-BI-mediated transport of HDL. Cell Metab. 17, 671–684.
Lipinski, C.A., et al., 2001. Experimental and computational approaches to estimate solubility and permeability in drug discovery and development settings. Adv. Drug Deliv. Rev. 46, 3–26.
Liu, D.M., et al., 2008. RNA interference mediated silencing of alpha-synuclein in MN9D cells and its effects on cell viability. Neurosci. Bull. 24, 96–104.

Liu, L., et al., 2012. Trans-synaptic spread of tau pathology in vivo. PLoS One 7, e31302.
Luo, H.M., et al., 2004. Down-regulation amyloid beta-protein 42 production by interfering with transcript of presenilin 1 gene with siRNA. Acta Pharmacol. Sin. 25, 1613–1618.
Magen, I., Hornstein, E., 2014. Oligonucleotide-based therapy for neurodegenerative diseases. Brain Res. 1584, 116–128.
Margulis, J., Finkbeiner, S., 2014. Proteostasis in striatal cells and selective neurodegeneration in Huntington's disease. Front. Cell. Neurosci. 8, 218.
Masliah, E., Spencer, B., 2015a. Applications of ApoB LDLR-binding domain approach for the development of CNS-penetrating peptides for Alzheimer's disease. Methods Mol. Biol. 1324, 331–337.
Masliah, E., Spencer, B., 2015b. Applications of ApoB LDLR-binding domain approach for the development of CNS-penetrating peptides for Alzheimer's disease. In: Langel, Ü. (Ed.), Cell-Penetrating Peptides. Springer, pp. 331–337.
Masliah, E., et al., 2000. Dopaminergic loss and inclusion body formation in alpha-synuclein mice: implications for neurodegenerative disorders. Science 287, 1265–1269.
McKeith, I.G., et al., 2017. Diagnosis and management of dementia with Lewy bodies: fourth consensus report of the DLB consortium. Neurology. 89, 88–100.
Morrison, H.W., Filosa, J.A., 2013. A quantitative spatiotemporal analysis of microglia morphology during ischemic stroke and reperfusion. J. Neuroinflammation 10, 4.
Mucke, L., Selkoe, D.J., 2012. Neurotoxicity of amyloid beta-protein: synaptic and network dysfunction. Cold Spring Harb. Perspect. Med. 2, a006338.
Overk, C.R., et al., 2014. Hippocampal neuronal cells that accumulate alpha-synuclein fragments are more vulnerable to Abeta oligomer toxicity via mGluR5–implications for dementia with Lewy bodies. Mol. Neurodegener. 9, 18.
Pardridge, W.M., 2016. Re-engineering therapeutic antibodies for Alzheimer's disease as blood-brain barrier penetrating bi-specific antibodies. Expert. Opin. Biol. Ther. 16, 1455–1468.
Pardridge, W.M., 2017. Delivery of biologics across the blood-brain barrier with molecular Trojan horse technology. BioDrugs. 31, 503–519.
Pardridge, W.M., et al., 1995. Human insulin receptor monoclonal antibody undergoes high affinity binding to human brain capillaries in vitro and rapid transcytosis through the blood-brain barrier in vivo in the primate. Pharm. Res. 12, 807–816.
Robertson, D.C., et al., 2004. Developmental loss and resistance to MPTP toxicity of dopaminergic neurones in substantia nigra pars compacta of gamma-synuclein, alpha-synuclein and double alpha/gamma-synuclein null mutant mice. J. Neurochem. 89, 1126–1136.
Rockenstein, E., et al., 2002. Differential neuropathological alterations in transgenic mice expressing alpha-synuclein from the platelet-derived growth factor and Thy-1 promoters. J. Neurosci. Res. 68, 568–578.
Sapru, M.K., et al., 2006. Silencing of human alpha-synuclein in vitro and in rat brain using lentiviral-mediated RNAi. Exp. Neurol. 198, 382–390.
Schluter, O.M., et al., 2003. Role of alpha-synuclein in 1-methyl-4-phenyl-1,2,3,6-tetrahydropyridine-induced parkinsonism in mice. Neuroscience 118, 985–1002.
Schoch, K.M., Miller, T.M., 2017. Antisense oligonucleotides: translation from mouse models to human neurodegenerative diseases. Neuron. 94, 1056–1070.
Selkoe, D.J., Hardy, J., 2016. The amyloid hypothesis of Alzheimer's disease at 25 years. EMBO Mol. Med. 8, 595–608.
Singer, O., et al., 2005. Targeting BACE1 with siRNAs ameliorates Alzheimer disease neuropathology in a transgenic model. Nat. Neurosci. 8, 1343–1349.
Soutschek, J., et al., 2004. Therapeutic silencing of an endogenous gene by systemic administration of modified siRNAs. Nature 432, 173–178.
Spencer, B.J., Verma, I.M., 2007. Targeted delivery of proteins across the blood-brain barrier. Proc. Natl. Acad. Sci. U. S. A. 104, 7594–7599.
Spencer, B., et al., 2009. Beclin 1 gene transfer activates autophagy and ameliorates the neurodegenerative pathology in alpha-synuclein models of Parkinson's and Lewy body diseases. J. Neurosci. 29, 13578–13588.
Spencer, B., et al., 2011. Peripheral delivery of a CNS targeted, metalo-protease reduces abeta toxicity in a mouse model of Alzheimer's disease. PLoS One 6, e16575.
Spencer, B., et al., 2013. Lentivirus mediated delivery of neurosin promotes clearance of wild-type alpha-synuclein and reduces the pathology in an alpha-synuclein model of LBD. Mol. Ther. 21, 31–41.
Spencer, B., et al., 2014a. ESCRT-mediated uptake and degradation of brain-targeted alpha-synuclein single chain antibody attenuates neuronal degeneration in vivo. Mol. Ther. 22, 1753–1767.
Spencer, B., et al., 2014b. A neuroprotective brain-penetrating endopeptidase fusion protein ameliorates Alzheimer disease pathology and restores neurogenesis. J. Biol. Chem. 289, 17917–17931.
Spencer, B., et al., 2015. A brain-targeted, modified neurosin (kallikrein-6) reduces alpha-synuclein accumulation in a mouse model of multiple system atrophy. Mol. Neurodegener. 10, 48.
Spencer, B., et al., 2016a. Reducing endogenous alpha-synuclein mitigates the degeneration of selective neuronal populations in an Alzheimer's disease transgenic mouse model. J. Neurosci. 36, 7971–7984.
Spencer, B., et al., 2016b. Alpha-Synuclein interferes with the ESCRT-III complex contributing to the pathogenesis of Lewy body disease. Hum. Mol. Genet. 25, 1100–1115.
Spencer, B., et al., 2016c. Systemic central nervous system (CNS)-targeted delivery of neuropeptide Y (NPY) reduces neurodegeneration and increases neural precursor cell proliferation in a mouse model of Alzheimer disease. J. Biol. Chem. 291, 1905–1920.
Spencer, B., et al., 2016d. A-synuclein conformational antibodies fused to penetratin are effective in models of Lewy body disease. Ann. Clin. Transl. Neurol. 3, 588–606.
Spencer, B., et al., 2018. Selective targeting of 3 repeat tau with brain penetrating single chain antibodies for the treatment of neurodegenerative disorders. Acta Neuropathol. 136, 69–87.
Stein, C.A., Castanotto, D., 2017. FDA-approved oligonucleotide therapies in 2017. Mol. Ther. 25, 1069–1075.
Suzuki, T., et al., 2006. Microglial alpha7 nicotinic acetylcholine receptors drive a phospholipase C/IP3 pathway and modulate the cell activation toward a neuroprotective role. J. Neurosci. Res. 83, 1461–1470.
Tai, Y., et al., 2014. Protective effect of alpha-synuclein knockdown on methamphetamine-induced neurotoxicity in dopaminergic neurons. Neural Regen. Res. 9, 951–958.
Takahashi, M., et al., 2015. Normalization of overexpressed alpha-Synuclein causing Parkinson's disease by a moderate gene silencing with RNA interference. Mol. Ther. Nucl. Acids 4, e241.
Tian, X., et al., 2015. LRP-1-mediated intracellular antibody delivery to the central nervous system. Sci. Rep. 5, 11990.
Ubhi, K., et al., 2010. Neurodegeneration in a transgenic mouse model of multiple system atrophy is associated with altered expression of oligodendroglial-derived neurotrophic factors. J. Neurosci. 30, 6236–6246.
Valera, E., Masliah, E., 2013. Immunotherapy for neurodegenerative diseases: focus on alpha-synucleinopathies. Pharmacol. Ther. 138, 311–322.
Valera, E., Masliah, E., 2016. Therapeutic approaches in Parkinson's disease and related disorders. J. Neurochem. 139 (Suppl. 1), 346–352.
Valera, E., et al., 2016a. Review: novel treatment strategies targeting alpha-synuclein in multiple system atrophy as a model of synucleinopathy. Neuropathol. Appl. Neurobiol. 42, 95–106.
Valera, E., et al., 2016b. Immunotherapeutic approaches targeting amyloid-beta, alpha-synuclein, and tau for the treatment of neurodegenerative disorders. Neurotherapeutics 13, 179–189.
Valera, E., et al., 2017. MicroRNA-101 modulates autophagy and oligodendroglial alpha-Synuclein accumulation in multiple system atrophy. Front. Mol. Neurosci. 10, 329.
Vossel, K.A., et al., 2010. Tau reduction prevents Abeta-induced defects in axonal transport. Science 330, 198.
Wang, T., et al., 2017. Challenges and opportunities for siRNA-based cancer treatment. Cancer Lett. 387, 77–83.
White, M.D., Mallucci, G.R., 2009. RNAi for the treatment of prion disease: a window for intervention in neurodegeneration? CNS Neurol. Disord. Drug Targets 8, 342–352.
Wolfrum, C., et al., 2007. Mechanisms and optimization of in vivo delivery of lipophilic siRNAs. Nat. Biotechnol. 25, 1149–1157.
Wunner, W.H., et al., 1984. Characterization of saturable binding sites for rabies virus. J. Virol. 50, 691–697.
Xilouri, M., et al., 2016. Impairment of chaperone-mediated autophagy induces dopaminergic neurodegeneration in rats. Autophagy 12, 2230–2247.
Yang, C.Y., et al., 1986. Sequence, structure, receptor-binding domains and internal repeats of human apolipoprotein B-100. Nature 323, 738–742.
Zharikov, A.D., et al., 2015. shRNA targeting alpha-synuclein prevents neurodegeneration in a Parkinson's disease model. J. Clin. Invest. 125, 2721–2735.